January 2014

Identification Of Novel Anti-Brain Tumor-Initiating Cell Compounds Using High-Throughput Screening

Garth William Strohbehn
Yale School of Medicine, garth.strohbehn@yale.edu

Identification of novel anti-brain tumor-initiating cell compounds using high-throughput screening

A Thesis Submitted to the Yale University School of Medicine in Partial Fulfillment of the Requirements for the Degree of Doctor of Medicine

By

Garth William Strohbehn, MPhil

2014

Abstract

Glioblastoma multiforme is the most common malignant primary intracranial tumor in adults. Despite years of advances in basic science knowledge about this disease including but not limited to cellular hierarchy, genetics, and mechanisms of proliferation and spread, overall survival of patients has remained unmoved for the past fifteen years, and long-term survivors are nearly nonexistent. Barriers to improved treatment occur in the realms of engineering and drug discovery: creation of an efficient delivery vehicle and identification of novel, efficacious small molecule compounds are necessary to achieve survival benefit in this disease.

In the following thesis, I describe efforts made by myself individually and alongside members of the laboratory of W Mark Saltzman, PhD, Goizueta Foundation Professor and Chairman of Biomedical Engineering, to test a novel, highly-penetrative polymeric nanocarrier platform for intracranial drug delivery and develop a high-throughput screen for small molecule compounds with efficacy against brain cancer stem cells. I show that the combination of the efficient delivery system and small molecule compounds with efficacy against brain cancer stem cells produces unprecedented gains in survival in a rat model of glioblastoma. Further, I describe the design and quality control methodology of the high-throughput small molecule screen and identify a large number of small molecule compounds with equal efficacy to first-generation anti-brain cancer stem cell drugs with fewer safety concerns. Together, the data underscore a) the promise of this efficient delivery vehicle to rapidly test the identified anti-brain cancer stem cell compounds and b) the potential for this combination to revolutionize glioblastoma therapy.

Acknowledgements

I am indebted to a number of folks for their efforts toward and support of this thesis. First and foremost, I thank my outstanding thesis advisor Professor W Mark Saltzman and associate research scientist-*cum*-Professor Jiangbing Zhou who has served as a mentor and a sounding board for many an enlightening conversation. Both of these gentlemen provided a critical eye and responsive sounding board during the development of this document. I am also indebted to Dr Tarek Fahmy for his helpful comments. Further, Dr Toral R Patel served as a wonderful mentor during my summers in the lab, and she along with Professor Zhou spearheaded this effort within the lab.

It has been a great pleasure to work with Professors Saltzman and Zhou for the past four years. Both have an approach to both science and management that I respect greatly: think of great interdisciplinary projects, recruit talented persons, and provide them with controlled autonomy.

A number of productive collaborations have developed out of this work. Fruitful collaboration with Professor Joseph M Piepmeier in the Department of Neurosurgery has catapulted this project to the next level. Collaboration with and pilot grant funding from the Yale Center for Molecular Discovery, in particular Drs Janie Merkel, Mariya Kolesnikova, and Pete Gareiss, have helped push this project forward. Finally, our recent collaboration with Professor Fahmeed Hyder and Drs Peter Herman and Daniel Comen in the Department of Diagnostic Radiology has been beneficial and leaves us well poised to translate this platform to the clinic.

Within the Office of Student Research, I have received an incredible amount of support, as well. Ms Donna Carranzo, Ms Mae Geter, and Dr John N Forrest provided outstanding institutional support throughout my five years at Yale. Additionally, I have been the recipient of fantastic financial support during my time at Yale – support that has afforded me the opportunity to travel throughout the United States and internationally discussing this work and learning more about advances in neuro-oncology.

I have been the recipient of generous funding provided by the Clinical and Translational Science Award TL-1 program, which supported my research year in 2011-2012, and the NIH, who provided stipend support to me during summer 2010 and experimental support for this project to Professor Saltzman over the course of the past four years. This work has been supported by grants to Professor Saltzman and company from, among others, the NIH, Chicago Institute of Neurosurgery and Neuroresearch Foundation, the Voices Against Brain Cancer Foundation, the B*Cured Foundation, the Yale Institute for Nanoscience and Quantum Engineering, and the Yale Center for Molecular Discovery.

I must mention numerous friends and, now, colleagues who I have turned to for fellowship and support throughout medical school, especially Ethan Dean, William Thomas Clarke, Mark Mai, Brooks Udelsman, and Daniel Wong. These gentlemen have proven themselves phenomenal men and exceptional thinkers, and I consider myself lucky to count them as friends. Finally, I am indebted to my labmates in the Saltzman lab, but especially Asiri Ediriwickrema and Drs Kofi-Buaku Atsina and Ben Himes.

Table of Contents

Introduction

Glioblastoma Multiforme: Epidemiology and Histology

Glioblastoma multiforme (more recently referred to as simply "glioblastoma" and, herein, "GBM") is the most common malignant primary intracranial tumor, with approximately 15,000 new cases each year [1]. The disease most commonly affects older non-Hispanic white male patients between the ages of 30 and 60 [2]. Patients most commonly present with headaches, development of seizure, and other complications related to mass effect rather than tumor [3]. GBM is suspected upon magnetic resonance imaging (hereafter "MRI") and is characterized by a deeply located, large, contrast-enhancing mass with central necrosis. The spatial distribution of GBM is most frequently frontal (40%) and temporal (29%); when accounting for brain volume this asymmetric distribution of origins remains pronounced [4]. Compared with low-grade gliomas, which are frequently peripheral, GBM is often found in deeper cortical locations, including the insula.

In contrast to metastatic tumors, World Health Organization classification of glial tumors is grade-only and is performed on a I-IV basis ([5]; Table 1). Tumors of both oligodendroglial (red print in Table 1) and astrocytic (blue print in Table 1) lineages occur and are indistinguishable on MRI. Within the oligodendroglial lineage, it is not at all uncommon for tumors to contain pockets of proliferative astrocytes. Accordingly, these lesions are named as a portmanteau of cell types: *oligoastrocytoma*. Only astrocytic lineage tumors have a grade I form; this lesion is most frequently found supratentorially in pediatric populations and is referred to as *pilocytic astrocytoma* for its hair-like projections and well-circumscribed

architecture. Grade II lesions are generally referred to as the *low-grade gliomas.* Within the astrocytic lineage, the lesion of note is diffuse astrocytoma – essentially, a pilocytic astrocytoma that has lost its well-circumscribed tissue architecture but does not contain overtly malignant cells. The oligodendroglial lineage is made up of oligodendroglioma or oligoastrocytoma and are infiltrative masses dominated by "fried egg" appearing oligodendroglial cells without mitoses. Grade III tumors generally have anaplastic features such as mitoses and hyperchromasia; accordingly, they receive the "anaplastic" descriptor. Whereas in the astrocytic lineage these tumors have no tissue-level malignant features like vascular proliferation (or endothelial proliferation, terms used interchangeably) or central necrosis, those in the oligodendroglial lineage are marked by vascular proliferation. Finally, grade IV tumors, GBMs, have characteristic histologic findings of necrosis and (*or,* in the case of astrocytic tumors) vascular proliferation.

There are thought to be two major pathways by which GBMs evolve, and are referred to as either *primary* or *secondary* GBMs [6-11]. Primary GBMs occur *de novo* typically in older patients and do not contain p53 mutations, whereas secondary GBMs occur in younger patients and are advanced tumors that have evolved from a low-grade glioma *in situ* and possess p53 mutations and often IDH1/2 mutations. GBMs with oligodendroglial components are uniformly IDH1 mutated with chromosome 1p/19q deletions.

GBM cells are highly migratory and transit through intercellular spaces, frequently crossing the midline via the corpus callosum. The end result is a highly disseminative but non-metastatic tumor. The near-universal recurrence GBM is also

notable for the site of recurrence: Often but not exclusively the tumor recurs in a 2cm radius from the periphery of the original tumor [12]. These two key features of GBM – the near-universal recurrence of disease and the highly invasive cellular component – have been neatly explained by invoking the *cancer stem cell hypothesis*.

A Brief History of the Cancer Stem Cell Hypothesis

Very briefly, the cancer stem cell hypothesis refers only to the hierarchy of cells present within a given tumor. Responsible for the initiation of each and every solid and liquid tumor is a cellular subpopulation – and ultimately a single cell – with features that are otherwise unique to *true* stem cells, among them self-regeneration, quiescence, and (at least) multipotency. The stem-like cell subpopulation of a tumor need not be a large fraction – often less than 1% in GBM [13] – but it is capable of driving invasion, angiogenesis, metabolic reprogramming, survival in fastidious conditions, and tumor growth in volume [14-17]. The consumptive component of the tumor – the bulk, terminally differentiated cellular component – is the largest contributor to tumor volume.

As mentioned earlier, cancer stem cells are used to explain tumor recurrence. While radiation and chemotherapy may appear to decrease a tumor's volume according to imaging studies, at least a share of cancer stem cells have survived by virtue of resistance. These surviving cancer stem cells then can repopulate the tumor, which now has resistance to the original chemotherapeutic drug. It therefore becomes clear that treatment of the disease with a single or, more likely, many compounds which have deleterious effects on cancer stem cells is necessary [18].

Of note, the cancer stem cell hypothesis does not seek to draw an absolute connection between normal stem cells and cancer stem cells. In the case of pediatric tumors, cancer stem cells may be derived directly from normal stem cells. In the case of adult tumors, however, it is much more likely for a terminally differentiated or transitional glial cell to acquire a single or set of oncogenic mutations which propels it toward a multipotent, stem-like state [19].

The Cancer Stem Cell Hypothesis in GBM

As discussed above, the cancer stem cell hypothesis has emerged as a possible explanation for chemotherapeutic and radiation resistance and, ultimately, tumor recurrence and patient's death [20]. In GBM, the cancer stem cell compartment has alternately been referred to as “brain cancer stem cells”, “brain cancer stem-like cells”, and “brain tumor-initiating cells”. Given that these same cells have features similar to primitive neural stem cells, we prefer “brain cancer stem cells” (hereafter, “BCSCs”) [21].

In all cases, this subpopulation shows capacity for asymmetric, self-renewing division and is (contentiously, [22]) shown to express CD133 (*prominin 1*) at its surface [23]. BCSCs are capable of a) establishing tumors *in vivo* from a small inoculum (<1,000 cells) that are histologically identical to the tumors from which they were isolated – complete with necrosis, vascular proliferation, and cellular atypia and mitotic figures. Further, BCSCs can proliferate and form neurospheres when grown *in vitro* in fastidious serum-free conditions [23], and this cellular subpopulation also expands under hypoxic conditions [17].

Many of the bulk properties of GBM can be explained by BCSCs. It has become increasingly clear that the BCSC subpopulation of GBM drives tumor progression, promotes angiogenesis, and influences tumor cell migration. *In vitro,* BCSCs are clearly resistant to both conventional chemotherapeutics [18], including carboplatin, cisplatin, paclitaxel, doxorubicin, vincristine, methotrexate, and temozolomide and radiotherapy [24] at clinically relevant dosages. Based on these *in vitro* studies, which employed excessively high concentrations of drug, it seems that *even if* conventional chemotherapeutics were combined with an ideal delivery vehicle (a challenge discussed later), better outcomes would not result.

Genetic Heterogeneity of GBM

Substantial genome sequencing and gene expression profiling has been performed on hundreds of GBM tumor samples, with the goal being identification of common thread genes or actionable pathways. What has emerged from this research is the insight that histologically identical GBMs can have very different genetic signatures (*intertumoral heterogeneity*) [7].

Four particular genetic subtypes have emerged from this line of research, termed neural, proneural, mesenchymal, and classical [25]. Acknowledgment of this knowledge is important going forward in the development of novel GBM therapeutics – it is now clear, based on this information and new information from a variety of cancer types, that efficacy of a given agent in a tumor is not guaranteed in its histologically identical counterpart.

GBM treatment – and indeed the treatment of every solid tumor – is further complicated by the genetic heterogeneity found within a tumor (*intratumoral heterogeneity)*. First explained in the context of renal cell carcinoma [26], it is now clear that cells isolated from distinct regions of a given GBM tumor bear grossly different expression signatures but appear to be descended from a common progenitor [27]. The exact explanatory power of the cancer stem cell hypothesis in this situation remains to be seen, as independent cancer stem cell subpopulations from distinct parts of GBMs have not been isolated and rigorously examined. What is clear, however, is that both *inter*- and *intra*tumoral heterogeneity must be explored and, possibly, accounted for in future drug discovery efforts.

A Brief History of GBM Therapeutics and Evolution of Outcomes

Despite years of research into molecular and cellular mechanisms as well as countless chemo- and radiotherapeutic trials, median overall survival times have remained near-constant since the introduction of radiation therapy [28]. Indeed, the oldest management method, surgery, is the single greatest determinant of extent of patient survival [2].

Originally, chemotherapeutic options included bis-chloroethylnitrosurea (also referred to as carmustine, BCNU, mustard gas, [29]) and the chemotherapeutic regimen of procarbazine, lomustine, and vincristine (also referred to as PCV, [30]) – both of these regimens utilize pre-1960s chemotherapeutics known to be untargeted, acting instead at the level of nucleic acid polymerization and dNTP synthesis. Intrathecal, intravenous, oral, and convection-enhanced methods of

chemotherapeutic delivery have been attempted in the past, and, not surprisingly, none produced substantial gains in overall survival in GBM [31]. Controlled-release delivery of BCNU in the form of the Gliadel® wafer had a small but significant benefit on survival [32-34]. First-generation chemotherapeutics, as well as Gliadel®, have proven beneficial in the treatment of low-grade glioma and anaplastic astrocytoma but have had only very limited benefit in the treatment of GBM. Delivery methods mentioned above, including issues raised by their failures, will be discussed later in the *Introduction*.

Most notably, GBM treatment went through a sea change in 2005 with the FDA's approval of temozolomide (trade name Temodar®). Temozolomide is a cytotoxic drug responsible for site-specific inhibition of methylguaninemethyltransferase [MGMT]; this specificity produces an improved side effect profile and roughly 25% benefit in median survival time as well as five-fold increase in long-term survivors when compared to placebo control [35, 36]. While MGMT hypermethylation is an independent predictor of survival in GBM, and radiation therapy improves outcomes in both hypermethylated and non-methylated MGMT promoter [37], temozolomide's survival benefit is seen in both types of tumors. However, the survival benefit of temozolomide administration is further magnified in tumors with hypermethylated MGMT promoters and resultant diminished MGMT expression [1, 37, 38]. Temozolomide, radiation therapy, and, most importantly, maximal surgical resection have subsequently become the backbone of every therapeutic regimen since. Dosing schedules of temozolomide are variable and highly customizable depending on clinical context.

More recent efforts have focused upon extending the use of anti-angiogenic therapy, namely anti-vascular endothelial growth factor monoclonal antibody *bevacizumab*, to GBM treatment. First approved by the FDA for recurrent GBM in 2009, bevacizumab has not been as efficacious as hoped; indeed, the European Union has not approved bevacizumab for GBM [39]. Bevacizumab, by virtue of decreasing vasculature, leads to an improvement in *imaging* results but no concomitant approval in survival. Necessarily, this leads to improvement in progression-free survival but no improvement in overall survival. More recently, up-front bevacizumab for newly diagnosed GBM has been tested in both US and European trials (RTOG0825 and Avaglio, respectively). Preliminary reports from these trials presented at the 2013 World Federation of Neuro-oncology Quadrennial Meeting suggest that there is zero overall survival benefit, but significant benefit in progression-free survival, as well as slower deterioration of Karnofsky Performance Status and longer time to initiation of steroid treatment with addition of bevacizumab.

There appear to be marginal benefits to addition of bevacizumab, mainly in the arena of quality of life, but at the level of the tumor there appear to be at least two substantial drawbacks to anti-angiogenic initiation. First, vascular permeability decreases with bevacizumab treatment, leading to even more difficult blood-brain barrier penetration. Second, evidence in other tumor types suggest an expansion of the cancer stem cell subpopulation in response to hypoxia [40]. Though this finding has not been duplicated in GBM and BCSCs, the idea merits further investigation.

Temozolomide is by conventional definitions a “good” drug, but it remains powerless to overcome GBM on its own. Indeed, despite years of honing and customizing current standard of care treatment (maximal safe surgical resection, radiation, and oral temozolomide), median survival following GBM diagnosis remains a dismal 14.6 months [35], and the five-year survival rate is less than 10% [41]. Discouragingly, the vast majority of GBMs recur within 2 cm of the original tumor focus [12].

What becomes clear from this overview is that 1) GBM has seen quite modest improvements in outcomes and 2) therapeutic insight has not flowed from scientific understanding. The failures of current GBM treatments has been attributed not to a lack of understanding of the disease process but to a lack of efficient, disseminated, and lasting drug delivery and the absence of chemotherapeutic drugs with efficacy against the relative cellular subpopulation [42]. Simply put, to date we have not made appropriate use of our knowledge.

GBM Treatment Challenges: Drug Delivery Problem and Potential Solutions

Nanocarrier-Mediated Drug Delivery in CNS Disease

Within the realm of drug delivery, one major obstacle to treating GBM is the blood-brain barrier [43]. The blood-brain barrier, while known to be weaker and more permeable in diseased states, largely prevents the entrance of highly polar and large chemical compounds into brain parenchyma. Indeed, the blood-brain barrier greatly limits the extravasation of compounds greater than 500 Daltons in molecular weight [44]. Additionally, polar compounds have been largely excluded. Small molecules

like temozolomide and carmustine are capable of crossing the blood-brain barrier, albeit inefficiently [45], but fail for both delivery- and cellular sensitivity-related reasons.

The blood-brain barrier can be bypassed altogether with direct, locoregional delivery of therapeutic agents either through catheter-based systems or implantation at the site of surgical resection. Initial work under this paradigm focused on the local implantation of a drug-loaded biodegradable polymer wafer (Gliadel®), which enables controlled release of carmustine over a prolonged period of time. However, the use of the Gliadel® wafer can only modestly improve GBM patient survival, typically by 2 months [34]. An experimental study suggested that, although these implants are able to achieve persistently high interstitial drug concentrations at the tumor site, there is poor drug penetration beyond the tumor margin, which thereby limits their efficacy [46]. Of course, in the design of these trials, patients are those who have failed multiple initial treatment regimens, including intravenous BCNU and PCV. That is to say, one potential reason for the relatively small survival benefit in these patients is the high likelihood that their tumors have acquired chemotherapeutic resistance from previous exposures, or a chemotherapeutic-resistant clone has come to predominate the bulk tumor population.

Polymeric wafer implants highlighted a second issue with contemporary therapeutics: the drug released from the wafer relies solely on passive diffusion to reach target cells. As a result, there is poor drug penetration of parenchyma outside of the tumor cavity [47-50]. Additionally, penetration of a distant tumor focus by the

small amount of free drug that *does* diffuse beyond the surgical margin is likely to be markedly decreased by the outward convective flow of fluid at the tumor periphery. The treatment of GBM would therefore be improved by strategies that a) enhance the depth of penetration of locally delivered therapeutic agents and b) overcome the problem of outward convective fluid flow.

Convection-enhanced delivery (hereafter, "CED") is a promising approach to overcome the limited distribution volume associated with diffusion-based delivery systems. For diffusion-based delivery, drug molecules move passively from regions of high concentration to regions of lower concentration. As a result, large molecules such as antibodies diffuse no more than 1 mm in 3 days, and small drugs that may have better diffusion are often quickly eliminated by capillary clearance or metabolism. In contrast, for dispersion using convection, agents are delivered to the brain via flow through a cannula under constant pressure. In this scenario, the dispersion of agents is powered by bulk flow kinetics or gradients of pressure, in addition to gradient of concentrations. As a result, it is possible to distribute agents widely in the brain.

Bobo and colleagues at the NIH first reported CED to the brain [51]. Since then, CED has been used in clinical trials, but this experience has revealed some limitations. Conventional CED of drug solutions results in an increased depth of penetration, but these results are transient. Free drugs are subject to high rates of elimination (i.e. they are diluted into cerebrospinal fluid or blood or taken up by capillaries) or they are high short half-lives in the brain: therefore, they disappear soon after the infusion stops [52]. This phenomenon could explain the failure of the recent

PRECISE trial, in which a potent targeted toxin, cintredekin besudotox (IL13-PE38QQR) in suspension, was delivered to brain tumors via CED but failed to show advantage when compared to diffusion-based Gliadel® wafers [53-55]. To overcome the limitations of CED, agents can be loaded into nanocarriers, such as liposomes, micelles, dendrimers or polymeric nanoparticles, which have small sizes to allow for distribution in brain, but can protect therapeutic agents from loss and control their release for long periods after infusion (Figure 2).

Nanoparticle delivery systems for drugs have been available for many years [56]. Many research groups focus on the use of nanoparticles introduced systemically, with the hopes that some of these particles will enter the brain through the BBB. This approach appears to work in some cases, although the percentage of intravenously administered particles that enter the brain is very low, with fewer 1% of particles entering the parenchyma, and the problems associated with diffusion-based delivery persist. It is not yet clear whether sufficient quantities of drug can be delivered by systemically-administered nanoparticles to make this a useful method for treating tumors in the brain (although there is some evidence nanoparticles may be useful for diagnostic purposes, such as iron oxide-containing nanoparticles that facilitate imaging of brain tumors [57]). An alternate, and we believe substantially more aggressive, approach is to deliver the nanoparticles directly into the brain, perhaps using CED to facilitate the distribution of the nanoparticles throughout the volume of the brain that needs therapy.

Polymeric nanoparticles can be delivered via CED to treat brain tumors. In a recent study, CED of camptothecin-loaded nanoparticles led to longer survival in animals

with intracranial tumors than CED of camptothecin alone [58]. However, prior efforts to deliver polymer nanoparticles via CED have achieved limited volume of distribution, due to large diameters that limit interstitial convective transport [58-60]. The pore size of normal brain interstitial space is between 40 and 60nm [61] while it is ~70-100 nm within a tumor in the brain [62]: these pore sizes suggest that nanoparticles for CED to intracranial tumors should be 60-80 nm in diameter, to leverage size-exclusion and allow for access to tumor-burdened parenchyma while limiting access to normal brain.

Development of Highly-Penetrative Polymeric Nanocarrier System

Central nervous system drug delivery took a large step forward with the development of the highly-penetrative polymeric nanocarrier platform by our laboratory in a parallel and complementary project [21, 63]. Invoking the concept of CED of polymeric nanocarriers capable of controlled release of drug payload, our laboratory has constructed a nanocarrier system composed of poly(lactic-co-glycolic) acid, the same FDA-approved co-polymer used in biodegradable sutures. When loaded with coumarin-6 fluorescent dye and injected into rat brains using CED, the nanocarriers disperse into a volume roughly four-fold larger than the volume infused. Compared to the smallest previously published nanoparticles, this represents a roughly two-and-one-half-fold increase in penetration. Further, the surface of the highly-penetrative polymeric nanocarrier system can be biochemically modified to contain ligands with activity in PET. When delivered in a porcine brain (a brain much larger than that of a rat but still smaller than that of a

human), the volume ratios remains a similar figure and, importantly, the nanoparticles can penetrate the all-important 2cm radius needed to prevent the majority of GBM recurrences. Altogether, these data show that 1) relatively widespread and clinically-relevant distribution of polymeric nanocarriers is possible and 2) real-time tracking of highly-penetrative polymeric nanocarriers is feasible. Finally, these findings show that the highly-penetrative polymeric nanocarrier system is an advantageous platform for rapid *in vivo* translation of candidate small molecule compounds and raise the possibility that if it were loaded with an appropriate compound, the system could help to prevent recurrence of GBM.

Imaging of Polymeric Nanoparticles

Accurate measurement of the distribution of a delivered agent is needed to assess drug or gene delivery in GBM. A number of methods have been employed; most relevant to our work are MRI and PET.

Drug distribution is quantified by MRI using gadolinium-based contrast agents [64]. Contrast provided by gadolinium agents, such as gadolinium-diethylene triamine pentaacetic acid (Gd-DTPA), can be used to monitor disruption of the blood-brain barrier [64], and when co-administered with a therapeutic agent or other macromolecule, can be used to directly assess the volume of drug delivery. Relevant to our work, gadolinium complexes have been encapsulated in polymeric nanocarriers, such as polymer nanoparticles for the purpose of studying drug

distribution [65]. This approach is appealing, but its accuracy may be limited by the release and additional diffusivity of gadolinium [66].

Positron-emission-tomography (PET) is another promising modality for imaging drug delivery to tumors, albeit a more expensive one than MRI. PET tracers can be infused concurrently with drug or bound to the delivery system, as shown in our highly-penetrative polymeric nanocarriers [21]. Overlaying PET with CT allows for anatomical assignment of drug distribution. Additionally, by virtue of using metabolically active amino acid tracers, PET may allow for finer resolution and more accurate estimation of the leading edge of the tumor [67, 68]. While PET certainly has advantages – and may well be useful as a one-time imaging study early in the therapeutic process – it remains an expensive, radiation-laden, and very short-lived technique [69]. For the purposes of following a polymeric nanocarrier over a time period relevant to its controlled-release kinetics, MRI is a superior methodology.

GBM Treatment Challenges: Drug Discovery

Automated HTS for Identification of GBM Treatments

Assuming the development of an ideal drug delivery vehicle that can be followed in real-time using non-invasive and non-destructive imaging techniques, we turn to the question of payload. As evidenced by the cellular and genetic complexity of GBM, an effective drug must be effective against not only a single BCSC population but also multiple, diverse BCSC populations. An effective compound must inhibit both arms of asymmetric cell division: the proliferation of GBM bulk tumor cells and the

self-renewal of BCSCs. In the event a compound does not kill BCSCs, it should promote their differentiation into bulk tumor cells, which are more readily killed by conventional chemotherapeutics (including temozolomide and carmustine) and, barring dedifferentiation [22], unable to spur tumor recurrence. Additionally, we should seek to identify compounds that have minimal deleterious effects against normal cellular populations, including neural stem cells and normal glial cells. Given the multiple cellular sensitivity requirements that must be met by a candidate anti-tumor compound, efficient discovery and clinical translation is a necessity. One such method of identification, as previously mentioned, is high-throughput screening. Broadly speaking, high-throughput compound screening is a system of consecutive methods reliant upon careful planning and design, large-scale preparation, small volumes measured using carefully calibrated nanoscale instrumentation, indirect measurement of effect (e.g. bioluminescence, fluorescence, or computer-assisted image interpretation used as a proxy for some property of the cell population), and large-scale statistical interpretation with the aim of discovering and quantitating the effects of candidate compounds on *something*. Within the context of drug discovery against a population of cells without a pre-defined molecular target, high-throughput screening often takes the form of exposing a characterized (and, optionally, immortalized) cell population to thousands of compounds of various classes (FDA-approved drugs, internationally-approved drugs, kinase and phosphatase inhibitors, natural products, or random chemical backbones) and subsequently analyzing cell number using bioluminescence, fluorescence, absorbance spectroscopy, or computer-assisted cell

counts after application of exogenous dye. In the case of a known molecular target, a similar but more indirect experiment can be performed with a different readout (e.g. fluorescence resonance energy transfer).

Given the obvious scientific and legal difficulties and expenses of shepherding a novel compound through all necessary pre-clinical testing and the FDA approval process, one of the goals of a high-throughput screening experiment is the identification of new functions for public domain compounds with known pharmacokinetics, pharmacodynamics, and toxicity, so called *repurposing*. Privately held compounds can be repurposed, as well. In the event that a novel chemical backbone is shown to have, for example, an anti-cancer effect, downstream synthetic and combinatorial chemistry can be performed to increase specificity and efficacy, as well as improve clinically relevant properties like half-life and solubility.

High-Throughput Screening Work Relevant to GBM

High-throughput screening projects aimed at therapeutic discovery have been undertaken in GBM, and, more specifically, BCSC and related systems. Initial efforts in the high-throughput screening of central nervous system disorders focused on identification of proliferation and self-renewal circuitry in mouse neural stem cells [70]. Building upon the broad functional similarities between neural stem cells and cancer stem cells (self-renewal and asymmetric division), a single primary mouse neural stem cell line was screened for growth in response to known pharmacologically active compounds. Follow-up screening focused upon the self-renewal capacity of cells pre-treated with growth inhibitory compounds as assessed

by neurosphere assay. This work, although an admittedly small screen, was important for its incorporation of normal glial cell control (mouse astrocytes), the insight that compounds thought to be previously innocuous (including *neurotransmitters*) could have broad effects on self-renewal, and the realization that high-throughput screening of stem cell populations was in fact feasible.

Most recently, and relevant to our project, eight small molecules were identified from a library of over 30,000 compounds [71]. The aim of this project was to identify compounds acting specifically at the level of BCSCs; therefore it utilized parallel screens of BCSCs and tumor matched bulk differentiated tumor cells. The weaknesses of this particular project were its lack of downstream characterization of compounds, an obvious inability to deliver the compounds (instead relying on pre-treatment inoculation models to "prove" *in vivo* activity), and lack of a normal cell population control (neural stem cell or normal glial cell). Most notable, however, is the lack of characterization of cell lines: the authors do not prove that these cell lines are different from one another or that the known intertumoral genetic heterogeneity of GBM is comprised between them, calling into question the therapeutic generalizability of their findings. That said, in addition to showing the feasibility of high-throughput screens in the context of cancer stem cells (a cell system with numerous technical challenges including slow growth, non-adherence, and expensive growth factor supplementation), the work is an important first step by virtue of its identification of compounds which could be repurposed for GBM treatment and for the use of an appropriate control (tumor-matched bulk tumor cell).

RNA interference, in the form of short interfering RNA (siRNA), is an in vogue experimental modality that specifically "knocks down" gene expression through delivery of a double-stranded RNA molecule that is ultimately processed into a single strand and binds to a complementary mRNA sequence. RNAi's use as a therapeutic modality is limited by expense, rapid degradation, and delivery, but its use as a research tool is undeniable. Within the realm of GBM and BCSCs, recent RNAi-based work has focused on identifying single kinases and phosphatases with effects on differentiation of BCSCs. This work builds on the insight that differentiating BCSCs and ridding them of their capacities for self-renewal and asymmetric division while also increasing sensitivity to apoptosis. The major weakness of this set of experiments is the limited number of genes being tested and, similar to the projects above, the lack of therapeutic proof for the identified gene and siRNA.

In recent work [72], we have performed a whole-genome siRNA screen on a characterized BCSC line in search of genes which, in response to decreased expression, lead to decreased stemness (as measured by *nestin* expression) and increased differentiation (as measured by *glial fibrillary acidic protein* expression and length:width ratio, a proxy for elongated mesenchymal phenotype of bulk tumor cells). The work is important for its scope and for the technical achievement of its use of automated imaging. What remains to be seen is the therapeutic role that these siRNA molecules can have going forward.

Altogether, these early successes suggest that high-throughput screening is a promising approach for identifying novel BCSC-targeted therapeutics. The intent of

this project is to focus upon small molecule screening, as it is clear that the universe of previously characterized chemical compounds has not been adequately vetted for its appropriateness in treating GBM or in eradicating BCSCs. We seek to build on previously developed high-throughput screening methods and combine these with development of a novel polymeric drug delivery platform.

In deciding on this pathway, Occam's razor is strictly applied: There may in fact be one compound that when delivered using a novel polymeric drug delivery platform substantially improves survival in GBM; a pervasive issue in GBM and central nervous system malignancy therapy has been drug delivery. Only once we are much more confident that the readily available resources (small molecule compounds) are not active on their own should we then progress toward combination therapy and introduction of biologics. Further the drawbacks of working with siRNA at this point in time are clear: Even if we could identify a single gene which reliably decreased expression of a critically important in BCSCs – and the identification of a single "master switch" for all BCSCs appears at first blush just as likely as identification of a small molecule compound which achieves the same end – issues of synthesis, delivery, regulatory approval, and cost present themselves as massive obstacles quite quickly. In short, there is no reason to introduce a new paradigm for GBM therapy when it has not clearly been shown to be necessary.

Hypotheses

In-House Small Molecule Screening

1) In-house screening will reveal previously- or currently-FDA-approved compounds with multiple modes of anti-BCSC activity.
2) Many of the drugs with anti-BCSC growth effect will also display the ability to differentiate BCSCs that are not killed and impair the self-renewal of BCSCs as assessed by flow cytometry and neurosphere formation assay, respectively.

Combining Anti-BCSC Compounds and Highly-Penetrative Polymeric Nanocarriers

3) We will successfully load the top candidate compound (as measured by lowest IC50 and successful promotion of differentiation and inhibition of self-renewal) into the previously developed highly-penetrative polymeric nanocarrier delivery vehicle.
4) Both highly-penetrative polymeric nanocarriers and top candidate compound will prove necessary but not sufficient to extend survival in rats burdened with BCSC-derived xenograft tumors. That is to say, CED of drug-only and nanocarrier-only solutions will provide zero survival benefit while drug-loaded nanocarriers will extend survival.

High-Throughput Screening of Anti-BCSC Small Molecule Compounds

5) We will develop a high-throughput assay utilizing multiple diverse BCSC lines that is highly accurate, highly reproducible, and free of systematic errors due to plating and diffraction of light.
6) By screening over 5,000 compounds for anti-BCSC activity, we will identify numerous previously- or currently-approved drugs that inhibit the growth of a genetically diverse set of BCSCs.
7) Compound-by-compound assessment will reveal certain shared chemical characteristics of novel anti-BCSC compounds. Evaluation of the known indications of these drugs will generate new testable hypothesis regarding both the mechanism of action of novel compounds in the setting of GBM and the etiology and pathogenesis of GBM.
8) There exist anti-BCSC compounds with only limited effects against normal cell populations. We will identify candidate compounds with equal *in vitro* efficacy as previously identified compound but with much more limited anti-normal cell population toxicity.

Pre-clinical Refinement of the Highly-Penetrative Polymeric Nanocarrier Platform for Magnetic Resonance Activity

9) We will successfully load citric acid-coated superparamagnetic iron oxide into highly-penetrative polymeric nanocarriers, and doing so will not impact the structural integrity of the nanocarriers.

10) *In vivo* testing of superparamagnetic iron oxide-loaded highly-penetrative polymeric nanocarriers will reveal that this formulation can be followed long-term by MRI and has similar distribution parameters as previously developed PET-avid and coumarin-6-loaded highly-penetrative polymeric nanocarriers.

Specific Aims

In-House Small Molecule Screening

1) We aim to, using low-throughput in-house screening methods, identify candidate drugs that have been previously approved by the FDA or international governing bodies with anti-BCSC effects as measured by growth inhibition.
2) We aim to characterize the *in vitro* effects of candidate drugs identified through large-scale in-house screening efforts on patient-derived glioma stem cell lines, as measured by neurosphere formation inhibition and differentiation status.

Combining Anti-BCSC Compounds and Highly-Penetrative Polymeric Nanocarriers

3) We aim to incorporate top candidate drugs into previously developed highly-penetrative polymeric nanocarriers.
4) We aim to test top candidate drugs formulated in highly-penetrative polymeric nanocarriers *in vivo* using a BCSC-derived model.
5) We aim to develop a high-throughput small molecule screening technique and verify its accuracy and precision.

High-Throughput Screening of Anti-BCSC Small Molecule Compounds

6) We aim to, using high-throughput screening methods, identify still more candidate drugs with anti-BCSC effects as measured by growth inhibition. By

virtue of screening multiple diverse BCSC lines, we aim to identify compounds with broad-based anti-BCSC effects.

7) We aim to identify structural characteristics common to many candidate drugs with anti-BCSC effects.
8) We aim to, using a counter-screening technique, identify anti-BCSC candidate drugs with limited effects against a normal glial cell population – thereby identifying drugs which will not only be efficacious but safe for clinical translation.

Pre-clinical Refinement of the Highly-Penetrative Polymeric Nanocarrier Platform for Magnetic Resonance Activity

9) We aim to prepare the highly-penetrative polymeric nanocarrier system for clinical translation by incorporation of superparamagnetic iron oxide.
10) We aim to test *in vivo* the stability and imaging properties of superparamagnetic iron oxide-loaded highly-penetrative polymeric nanocarriers.

Methods

Chemicals

All chemicals, including all drugs screened in in-house screening, were purchased from Sigma-Aldrich unless otherwise noted. Dithiazanine iodide was purchased from Sigma-Aldrich, as were ethyl acetate, dichloromethane, polyvinyl alcohol, trehalose, and dimethylsulfoxide. Poly-lactic-co-glycolic acid was purchased from Polysciences, Inc.

BCSC cultures

Tumor samples classified as GBM based on World Health Organization criteria were obtained from neurosurgical patients at Yale-New Haven Hospital who had provided informed consent preoperatively (HIC Protocol #0802003495). BCSCs were isolated in the following manner. Within 1 to 3 hrs of surgical removal, tumors were washed, cut into <1 mm^3 fragments, and enzymatically dissociated into single cells. Digested fragments were filtered using a 70 μm cell strainer (BD Falcon) and collected in culture medium. The GS5 cell line was kindly provided by Lamszus lab [73]. All primary tumor cells were collected and cultured in Neurobasal A medium (Invitrogen) supplemented with B27 (Invitrogen), fibroblast growth factor-2 (20 ng/mL, Peprotech), and epidermal growth factor (20 ng/mL, Peprotech). Growth factors were added at least weekly. Non-adherent cells growing as spheres were passaged as necessary and to maintain purity. All members of the Saltzman lab, but most notably Professor Jiangbing Zhou and Dr Toral Patel, developed cell lines named in the convention “PS##”.

Cell culture

All BCSCs were cultured in Neurobasal A medium (Invitrogen; Carlsbad, CA) supplemented with B27 (Invitrogen), 100 ng/uL EGF (Peprotech; Rocky Hill, NJ), 100 ng/uL FGF (Peprotech), and penicillin/streptomycin/fungizone (Lonza; Walkersville, MD). The human glial cell line SVGp12 (ATCC; Manassas, VA) was used as a safety control. SVGp12 was cultured in Minimal Essential Medium (Invitrogen) supplemented with fetal bovine serum (Atlanta Biologicals; Lawrenceville, GA) and penicillin/streptomycin/fungizone (Lonza). The author and all members of the Saltzman group performed BCSC culture.

Drug Compounds for Screening

Over 1,000 compounds were screened in-house. This collection was comprised of components that at one time or another were FDA-approved.

Compound collections screened in high-throughput screening included: NIH Clinical Collection (NIH; Bethesda, MD), Pharmakon 1600 (Microsource; Gaylordsville, CT), Ion Channel Inhibitors (Enzo; Farmingdale, NY), Kinase Inhibitors (Enzo), Phosphatase Inhibitors (Enzo), Metabotropic & Glutamatergic Ligands (Enzo), and FDA-approved drugs (Enzo). The author, in consultation with Professor W Mark Saltzman, Professor Zhou, and collaborators at the Yale Center for Molecular Discovery selected all compound libraries for screening.

Cell proliferation assays

For primary screening, a slightly modified MTT assay was used to quantify the effects of drugs on cell proliferation. Briefly, cells were cultured in 96-well plates (Falcon). 6 days after treatment, media was removed and replaced with fresh media containing 10% MTT (3-(4,5-dimethylthiazol-2-yl)-2,5-diphenyl tetrazolium bromide) (Sigma) solution (4.14 mg/mL). Four hours after incubation at 37ºC, all media was removed. Formazan was dissolved in DMSO and the optical density (O.D.) was measured at 590 nm. The relative inhibition on growth was determined using the following formula:

$$Growth\ Inhibition = \frac{Optical\ density_{control} - Optical\ density_{experimental}}{Optical\ density_{control}}$$

Proliferation was also assessed and IC50 calculated using AlamarBlue (Invitrogen) fluorescence. Briefly, cells were plated at subconfluent concentration in black clear-bottomed 96-well plates (Falcon) with drug concentrations spanning eight orders of magnitude. Three days post-plating, AlamarBlue was added at manufacturer's recommended concentration. Cells were incubated at 37ºC for 200 min and quantified (ex: 544 nm, em: 590 nm). Fluorescence measures were corrected for background media and drug fluorescence and normalized to the mean of vehicle measures. IC50 values were determined using four-parameter logistic modeling using normalized point estimates. The author and Professor Zhou performed all cell proliferation assays.

Spheroid formation assay

BCSCs were plated as single-cell suspensions of 5 cells per μL in 48-well plates (Falcon). Cells were treated with 1 μM drug or equivalent concentration of DMSO. Growth factor was supplemented on day 5. Wells were counted on day 7. Colonies containing more than 5 cells were considered to be spheres. Percent inhibition was calculated as:

$$Percent\ Inhibition = \frac{(Spheres_{control} - Spheres_{experimental})}{Spheres_{control}}$$

The author performed all spheroid formation assays.

Flow cytometry

BCSCs were plated as single-cell suspensions in 6-well plates with 100 nM drug or DMSO. 3 days after plating, suspensions were collected and flow cytometry performed. Briefly, following reconstitution in 0.5% BSA in PBS (w/v), dissociated cells were washed in cold PBS and subsequently incubated with biotin-conjugated anti-CD133 (PROM1) antibody (Miltenyi Biosciences). Suspensions were incubated with avidin-conjugated AlexaFluor 488 (Invitrogen) and read on a BD FACSCAN flow cytometer (BD Biosciences). Geometric means were calculated in FlowJo (TreeStar, Inc.), corrected for background (secondary only), and normalized to DMSO-only treated cells. The author performed all flow cytometry studies.

Ultrasmall Nanoparticle Synthesis (Figure 1)

Nanoparticles loaded with dithiazanine iodide were synthesized by a single-emulsion solvent evaporation technique. 100 mg poly-lactic-co-glycolic acid (50:50, Polysciences and Birmingham) and agents to be encapsulated were dissolved in 2 mL dichloromethane or ethyl acetate. The polymer/drug solution was then added dropwise to 4 mL 2.5% polyvinyl alcohol as the outer aqueous phase and sonicated to form an emulsion. The emulsion was poured into a beaker containing aqueous 0.3% (v/v) polyvinyl alcohol and stirred at room temperature for 3 hours (dichloromethane as solvent) or 5 hours (ethyl acetate as solvent) to allow solvent to evaporate and particles to harden.

To synthesize standard-sized nanoparticles, following the solvent evaporation phase, the nanoparticle solution was subjected to typical centrifugation speeds (11,500 x g for 15 minutes, x 3) and the pellet was collected. To synthesize ultrasmall nanoparticles, following the solvent evaporation phase, the nanoparticle solution was first centrifuged at low speed (8,000 x g for 10 minutes) to pellet the large particles. Supernatant was decanted and ultrasmall nanoparticles were collected through high-speed ultracentrifugation (100,000 x g for 30 minutes, x 2). To prevent nanoparticle aggregation during lyophilization, trehalose was added to the final aqueous solution at a ratio of 0.5:1 (trehalose:nanoparticles) by mass immediately prior to lyophilization. Professor Zhou and Dr Patel performed nanoparticle synthesis.

Antitumor activity in xenograft model

To establish tumors for evaluation of paclitaxel-loaded PLGA nanoparticles, nude rats were first anesthetized with a ketamine/xylazine mixture. Animals were then prepped with betadine and alcohol and placed in a stereotactic frame. A linear midline incision was made and a 1.5 mm diameter hole was drilled in the skull 3mm lateral and 0.5 mm anterior to bregma. A 26G Hamilton syringe was inserted to a depth of 5mm. The tissue was allowed to equilibrate mechanically for 2 minutes. Subsequently, $5x10^5$ GS5 cells in 2 μL PBS were injected into the brain over 10 minutes. The burr hole was filled with bone wax (Lukens, Reading PA), the scalp closed with surgical staples, and the rat removed to a clean cage with free access to food and water mixed with ibuprofen. Treatments were performed 10 days following tumor inoculation. Rats were again anesthetized, prepped, and placed in a stereotactic frame. The wound was reopened and the Hamilton syringe was oriented as described previously. 20 μL of either nanoparticles (100 mg/mL) or free drug (either 60 μg or 120 μg) were infused continuously at a rate of 0.667μL/min. Equilibration was performed and animals were handled post-operatively as described. The animals' weight, grooming, and general health were monitored on a daily basis. Animals were euthanized after either a 15% loss in body weight or when it was humanely necessary due to clinical symptoms. Professor Zhou and Dr Patel performed the above procedures.

High-Throughput Screening of BCSCs (Figure 2)

In collaboration with the Yale Center for Molecular Discovery, we optimized a fluorescence-based high-throughput assay for identification of anti-BCSC compounds. We performed primary screening of ~5,000 compounds of varying origins (kinase/phosphatase inhibitors, internationally-approved compounds, FDA-approved compounds, etc.) for anti-BCSC growth activity. Briefly, assays were performed in 384-well black plates. GS5, PS16, and PS30 cells were cultured in the manner described previously in T150 flasks. Cells were seeded in 384-well black-well, clear-bottom plates at a density of 2,000 cells per well either by multichannel pipette or multidrop (Thermo Scientific) in total volume. 24 hours later, compound was added to a concentration of 8 μM using a sterilized PlateMatePlus transfer apparatus (Matrix Technologies). Following 3 day incubation at 37C, cell viability was determined using the mitochondrial redox assay AlamarBlue (Invitrogen) as above. Fluorescence intensity (λ_{ex} = 544 nm; λ_{em} = 590 nm) was determined using an Envision plate reader (PerkinElmer).

Compounds were rank-ordered according to their percent mortality effect on the various BCSC lines. The top 100 compounds were identified and subsequently screened against the normal human glial cell line SVGp12 using similar conditions as the primary screen. The author, in collaboration with the Yale Center for Molecular Discovery, developed, validated, and carried out all high-throughput screening methods.

Synthesis of superparamagnetic iron oxide

Superparamagnetic iron oxide (SPIO) synthesis and coating with oleic acid, oleylamine, and 1,2-hexadecanediol proceeded according to Ragheb et al, 2013 [74]. Black solution was precipitated in 100% ethanol, washed twice, and dried to form a black powder. Professor Zhou performed SPIO synthesis.

Encapsulation of superparamagnetic iron oxide in highly-penetrative polymeric nanocarriers

Reaction conditions for highly-penetrative polymeric nanocarrier synthesis were the same as described above. Superparamagnetic iron oxide prepared as above was added to single emulsion reaction mixture along with coumarin-6 in ethyl acetate to final concentrations ranging from 0.25mg/20μL to 2mg/20μL. The polymer/superparamagnetic iron oxide solution was then added dropwise to 4 mL of 2.5% polyvinyl alcohol as the outer aqueous phase and sonicated to form an emulsion. The emulsion was poured into a beaker containing aqueous 0.3% (v/v) polyvinyl alcohol and stirred at room temperature for 3 hours (dichloromethane as solvent) or 5 hours (ethyl acetate as solvent) to allow the solvent to evaporate and the particles to harden.

To synthesize ultrasmall nanoparticles, following the solvent evaporation phase, the nanoparticle solution was first subjected to low-speed centrifugation (8,000 x g for 10 minutes) to pellet and remove the large particles. The ultrasmall nanoparticles remaining in the supernatant were subsequently collected through high-speed ultracentrifugation (100,000 g for 30 minutes, x 2).

To prevent nanoparticle aggregation during lyophilization, trehalose was added to the final aqueous solution at a ratio of 0.5:1 (trehalose:nanoparticles) by mass immediately prior to lyophilization.

Nanoparticles were injected into rat brain parenchyma using CED as described in the section *Antitumor activity in xenograft model.* The author, Professor Zhou, neurosurgery resident Dr Komli-Kofi Atsina, and the Diagnostic Radiology team of Dr Peter Herman and Dr Daniel Coman performed these studies.

MRI of rats injected with superparamagnetic iron oxide-loaded highly-penetrative polymeric nanocarriers

In collaboration with MRI Research Center, rats were anesthetized using isoflurane and loaded into 9.2T small animal MRI. A second set of experiments was performed in a 4T small animal MRI. Sixteen coronal images were collected for each rat using proprietary software. Vitals were monitored throughout imaging. The Diagnostic Radiology team of Dr Peter Herman and Dr Daniel Coman performed these studies with the author's assistance.

Statistical analysis of High-Throughput Screen

All data were taken in triplicate and reported as mean and standard deviation. Comparison of two conditions was evaluated by a paired Student's t-test. Kaplan-Meier analysis was employed to evaluate the effect of various treatments on survival. A $p \leq 0.05$ was considered to indicate a statistically significant difference. Initial quality control analysis of high-throughput screening data was performed

using Z'-factor statistic, a reliable measure of the difference between true positive and true negative controls [75]. Z'-factor is calculated according to the formula:

$$Z' = 1 - \frac{(3\bar{\sigma}_E + 3\bar{\sigma}_S)}{|\bar{y}_E - \bar{y}_S|},$$

where *E* refers to positive control samples (the previously identified compound anisomycin), *S* refers to negative control samples (in our case, the vehicle control DMSO), σ refers to standard deviation, and $\bar{y}$ refers to mean fluorescence signal. Z' is interpreted as 1 being ideal, >1 being impossible, 0.5-1 being an excellent assay, 0.25-0.5 as being a good and acceptable assay, <0.25 as being a marginal to poor and unacceptable assay. The author performed statistical analyses.

Results

Identification of novel small molecules that inhibit BCSC proliferation and self-renewal

Tumor cell heterogeneity and resistance are significant obstacles that must be overcome to cure GBM – BCSCs must be eliminated. Given that BCSCs are known to resist standard chemotherapy drugs, including paclitaxel, novel small molecules that inhibit the growth of BCSCs must be identified (Fig. 3a). We therefore screened a library of ~2,000 compounds that at one time or another have been approved for use in humans by the FDA for growth-inhibitory activity against GS5. Briefly, GS5 cells were plated in 96-well format, treated with 5 μM drug, and evaluated for viability three days later using MTT. Initial hits were subsequently evaluated for inhibition of GS5 sphere formation, a measure of BCSC self-renewal. Selection criteria included both growth inhibition and sphere formation inhibition of ≥ 50% (Fig. 3a).

Thirty-two candidate compounds were identified (Table 2), only 3 of which were confirmed in a high-throughput screen in BCSCs (Visneyi ref). The BCSC growth-inhibitory activity of many compounds was confirmed using AlamarBlue. One compound in particular, the anti-helminthic cyanine dye dithiazanine iodide, potently inhibited GS5 proliferation with an IC50 of 79 nM. Dithiazanine iodide inhibited GS5 sphere formation, a measurement of BCSC self-renewal, by 93.6%. Additionally, dithiazanine iodide decreased the CD133+ cell population by 56.6% in treated cultures. Dithiazanine was also evaluated in two additional BCSC lines

isolated in our lab, PS11 and PS16, and showed similar anti-BCSC effects in both (Fig 3b).

Follow-up studies of other top candidate compounds, including emetine (the top-ranked compound from UCLA screen), acriflavine, and digoxin, indicate limited growth inhibitory effects against BCSCs and bulk tumor cells in normal oxygen atmosphere and BCSCs under hypoxic conditions (Table 3) with high potency (Table 4). As expected, emetine showed high efficacy and potency under all conditions, in line with previously reported data from Visnyei, *et al.* Notably, emetine and digoxin were routinely at least twice as potent as acriflavine. Routinely, digoxin displayed lower efficacy than acriflavine and emetine, suggesting that even if high levels of drug could be delivered to the site of the tumor, only minimal BCSC killing would occur. Additionally, the lone bulk tumor cell line used, U87, showed profound resistance to digoxin, suggesting that if this drug were to be used as a chemotherapeutic for GBM, it would need to be combined with a known bulk tumor cell-inhibiting agent such as BCNU, PCV, or temozolomide.

CED of ultrasmall, dithiazanine iodide-loaded PLGA nanoparticles for GBM therapy

Toward development of an efficacious, translatable therapy for GBM, we sought to assess whether CED of ultrasmall, DI-loaded nanoparticles could prevent the growth of BCSC-derived xenografts. Since the ultrasmall nanoparticles can penetrate over a large volume of brain parenchyma, we hypothesized that CED of ultrasmall,

dithiazanine iodide-loaded nanoparticles would have an unprecedented advantage in treating these disseminated tumors.

To evaluate their efficacy *in vivo*, ultrasmall, dithiazanine iodide-loaded nanoparticles were administrated into rat brains bearing tumors derived from GS5 using the same procedures described previously. As shown in figure 4, DI nanoparticles significantly increased survival of tumor-bearing rats; these rats have been alive for over nine months. Professor Zhou and Dr Patel carried out these studies.

High-throughput screening assay: Quality control

There are three characteristics of high quality high-throughput assays: the ability to distinguish positive and negative results and be relatively free of systematic errors such as row and column effects. The high-throughput assay as constructed has strong Z' scores (Fig. 5e), a statistical measure of the difference between positive and negative results. Z' score greater than 0.5 is considered excellent and is industry standard – it is interpreted as being a 12 standard deviation difference between true positive and true negative controls. Distinguishing row and column effects is purely observational, and no clear industry standard exists for statistical evaluation. Compared to previously developed assays [76] our assay displays less variability when binned rows of 384-well plates (Fig. 6a-c).

High-throughput screening assay: Identification of Candidate Anti-BCSC Compounds

Using a fluorescence-based methodology, cell growth inhibitory effects of compounds were assessed. Compounds with anti-growth activity against one BCSC line tended to be highly efficacious in other BCSC lines (Fig. 7a). That is to say, if a compound were efficacious against one cell line, it was likely efficacious against all cell lines. Further investigation of signal inhibition showed that over 200 compounds had greater than 50% cell growth inhibitory power in at least one BCSC line (Fig. 7b). PS16 cells appeared the most sensitive to tested drugs, with PS30 and GS5 being substantially less so. Ninety-nine compounds with greater than 50% inhibitory effect against all BCSC lines were identified (Fig. 7b). Compared to previously published exploratory small molecule screens, the percentage of compounds with anti-growth efficacy is high, largely owing to the fact that our libraries are biased toward inclusion of anti-growth drugs. For follow-up experimental convenience, compounds were ranked according to their mean anti-growth efficacy across the three cell lines. Three hundred twenty compounds were selected for repeat screening in BCSCs and counter-screening against normal glial cells SVGp12 (Fig. 7c).

High-throughput screening assay: Counter-screening of candidate compounds for glial cell toxicity

As discussed previously, our earlier low-throughput screening efforts identified dithiazanine iodide as a strong candidate anti-BCSC drug. One issue with

dithiazanine iodide, however, is its history of systemic toxicities [77]. Furthermore, in-house evaluation of dithiazanine iodide showed toxicity against the normal glial cell line SVGp12 (Fig. 8a). Dithiazanine iodide displays high activity, with nanomolar IC50, and near 100% efficacy at micromolar doses. In the interests of finding a compound with anti-BCSC efficacy but without toxicity against SVGp12, the top 320 compounds from primary screening were "counter-screened" against SVGp12 in duplicate with the goal of identifying safe, efficacious compounds for GBM treatment.

Anti-BCSC and anti-glial cell data were collected and expressed as efficacy. Instructive for data viewing is to plot the anti-glial "efficacy" for a given compound versus its mean anti-BCSC efficacy (Fig. 8b). Twelve compounds were found to have anti-BCSC efficacy greater than dithiazanine iodide, and 49 compounds had greater anti-BCSC efficacy than our previously identified positive control anisomycin (Table 5, red diamonds in Fig. 8b). Five of the twelve compounds had substantially less anti-glial cell toxicity: mitoxantrone, emetine, quinacrine, pyrithione, benzalkonium chloride, and benzethonium chloride.

Side-by-side comparison for a given drug of anti-BCSC anti-glial cell efficacy displays the differences well (Fig. 8c). Increased difference between the two efficacy values indicates a relative preference for efficacy against one cell type. This graph makes clear that we have identified compounds with *in vitro* anti-BCSC efficacy as high as the best previously identified (and *in vivo*-confirmed) small molecule drug but with less anti-glial cell toxicity.

In vivo MRI of superparamagnetic iron oxide-loaded nanoparticles

Following loading of superparamagnetic iron oxide into highly-penetrative polymeric nanocarriers, CED of nanoparticles in normal rat brain was performed using methods described above. Varying doses of superparamagnetic iron oxide were utilized in these experiments, ranging from 0.25mg/20μL to 2mg/20μL. Early experiments using high-concentration SPIO (2mg/20μL) were successful insofar as contrast signal remaining in brain parenchyma for one month. The weakness of high dose-SPIO was that intensities recorded immediately post-infusion were beyond the upper limit of detection ("blown out" or "saturated"). An eight-fold reduction in SPIO concentration to 0.25mg/20μL produced T2 MRI signal that remained for one month (Fig. 9c-d) and but was saturated on initial imaging (Fig. 9a-b).

Initial observation suggested that a pocket of non-nanoparticle-containing infusate had collected, and prior experience suggested this was secondary to the 20μL volume used. To estimate the effect of infusate volume on short- and long-term signal, one rat was infused with an equal concentration of SPIO albeit in a 10μL volume. Initial imaging results showed that a decrease in non-signal bubble (Fig. 9f). As expected, at time of infusion, MR signal intensity was not saturated (Fig. 9g-h), and the contrast signal was present for up to one month (Fig. 9i-j).

While not measured directly, we expect premature release of gadolinium to play only a minor role in these results, as the half-life of gadolinium in cerebrospinal fluid has been previously reported as approximately between 8.5 hours in stroke studies, albeit with a different formulation [78]. Modified superparamagnetic iron oxide (e.g. with dextran coating) tends to have longer plasma half-life (on the order of 14-30

hours) due to slower opsonization and clearance from the blood pool [57]. Together, these data show that superparamagnetic iron oxide can be loaded into highly-penetrative polymeric nanocarriers without affecting morphologic characteristics and distribution properties and can be followed using T2 MRI over at least a month-long period of time.

Discussion

In this thesis, I explain in detail one-half of the development of a potential therapeutic for the treatment of GBM. Overall, this novel therapeutic addresses the two most commonly cited obstacles to effective therapy: 1) the infiltrative nature of GBM tumors and 2) the genetic heterogeneity of the tumor and chemoresistance of BCSCs, which give rise to drug delivery and discovery challenges, respectively. Additionally, I discuss further the impact of high-throughput screening against multiple genetically diverse BCSC lines, the role of counter-screening against a normal cell population, and the development of a MR-compatible delivery vehicle. Altogether, I will show the clinical readiness of this new and exciting therapeutic modality.

Impact of the highly-penetrative polymeric nanocarrier delivery vehicle

To overcome the challenges associated with drug delivery, we developed a controlled-release delivery system comprised of ultrasmall poly-lactic-co-glycolic acid nanoparticles that can penetrate substantially (~ 7-fold) higher volumes than conventional poly-lactic-co-glycolic acid nanoparticles when delivered intracranially using CED. It was also encouraging to note that the V_d/V_i achieved in rodent studies were comparable to those achieved with nanoliposomal delivery systems [79]. Highly-penetrative polymeric nanocarriers delivered in pig brains using CED penetrated into volumes of approximately 1179 mm^3. Since the vast majority of GBM tumors recur within 2 cm of the original tumor focus [12], the penetrative

capacity of these ultrasmall nanoparticles delivered by CED may sufficiently address the infiltrative nature of GBM in future clinical application.

In comparison to currently available nanocarrier drug delivery systems, this platform has at least three clear advantages. First, the polymer has an excellent safety profile: poly-lactic-co-glycolic acid was approved by the Food and Drug Administration (FDA) in 1969 and has safely been used in clinics since that time. Second, the release kinetics of these nanoparticles can be more easily modulated than those of competing nanocarrier systems utilized in intracranial applications, namely liposomes and micelles. Third, the versatile surface modification approach described previously enables rapid, modular attachment of biotinylated agents, thereby allowing for efficient labeling of nanoparticles with a host of cell-targeting and -penetrating agents. Finally, the exceptionally small diameters allow these nanoparticles to penetrate relatively large, clinically relevant volumes when delivered by CED – irrespective of whether it is infused through tumor-burdened brain or normal parenchyma. In short, this is a delivery system with the potential for significant utility.

Although the highly-penetrative polymeric nanocarrier delivery vehicle was evaluated using treatment of intracranial tumors with small molecule compounds as a test case, the system could easily be tailored for application to a host of central nervous system disorders. For example, surface modification or size fractionation could produce particles well suited for the treatment of neurodegenerative disorders. Additionally, these particles have the potential to encapsulate not only

hydrophobic drugs but also a variety of nucleic acids for gene therapy applications [63].

Impact of anti-BCSC drugs

BCSC resistance to conventional chemotherapeutics is a major challenge toward effective GBM therapy. To facilitate discovery of small molecule drugs with the ability to inhibit the growth and self-renewal of BCSCs, a low-throughput, in-house library screening approach was first used successfully. Approximately 2,000 compounds that have been, at one time or another, FDA-approved were tested for the aforementioned abilities. 32 lead compounds were identified and subjected to further testing. We originally settled upon the anti-helminthic cyanine dye dithiazanine iodide for its abilities to inhibit growth and self-renewal and differentiate cells it fails to kill. Adding credibility to our screening protocols are relatively recent reports confirming many of our identified drugs using both high-throughput [UCLA] and small-scale approaches [80, 81].

Identified compounds also appear to be largely generalizable based on preliminary and follow-up work. Our in-house screen identified compounds, including dithiazanine iodide, with growth inhibitory, self-renewal-inhibitory, and pro-differentiation effects against multiple diverse BCSC lines. Based on prior work by The Cancer Genome Atlas working collective, each cell line tested serves as a proxy for a different subtype of GBM. Our early results suggest that dithiazanine iodide is a generalizable option for anti-BCSC-directed GBM therapy. Dithiazanine iodide has anti-growth, anti-self-renewal, and differentiating effects on BCSCs – but the extent

with which these latter two characteristics would in practice have an effect therapeutically remains to be seen. The remainder of our work focuses upon growth inhibition as a proxy for *in vivo* efficacy.

Previous work in humans showed dithiazanine iodide to have significant nephrotoxicity when delivered by parenteral route, and subsequent work identified dithiazanine iodide as being significantly cytotoxic against normal human glial cells, raising questions about not its effectiveness but its safety. Granted, in an ethics discussion of whether to move forward with a compound, certain costs and benefits must be weighed, and it is likely that if no other drug worked *as well* as dithiazanine iodide and were simultaneously *safer*, we would of course move forward with translation of dithiazanine iodide. The point, however, remains that we owe it to research subjects – and future patients – to do due diligence to the best of our abilities in the search for the most efficacious and safest candidate drugs.

As there are myriad compounds not contained within our set that may have anti-BCSC effects, it was important to increase the volume of our test set. Doing so, however, requires new methodologies in order to be both cost-effective and rapid. High-throughput screening has proven itself as a rapid, accurate, and precise method of drug discovery.

We are one of the first to develop a rapid, reproducible, and accurate high-throughput assay in a cancer stem cell line. We are the first to perform said screen in multiple diverse cancer stem cell lines, thus showing that despite differences in genetic programming, BCSC line isolated from multiple distinct tumors, at least in terms of drug sensitivity, are far more similar than they are different. This insight

raises the possibility of indeed finding a "silver bullet" treatment for GBM, provided the correct level of the cellular hierarchy, rather than the correct *protein* or *gene*, can be targeted.

Compounds identified to have anti-growth efficacy against all BCSC lines were diverse, and it appears unlikely from initial pharmacogenomics that all compounds affect a final common pathway. Candidate drugs are not without their similarities, however. Interestingly, seven of the top 30 compounds with anti-BCSC efficacy and limited anti-glial cell toxicity contain a cationic quaternary ammonium complex. This novel finding, combined with the known *in vivo* efficacy of dithiazanine iodide, suggest that quaternary ammonium compounds and anti-helminthic compounds could play a role in stunting tumor propagation. Furthermore, it may suggest an infectious role for pathogenesis and propagation of GBM.

The role of safety controls – normally-occurring human cell populations – in high-throughput screens has been discussed before. Indeed, a number of projects have either relied on counter screens or on direct screening of normal populations to identify novel therapeutics [70, 71, 82-85]. The extent to which *in vitro* toxicity mimics or can predict *in vivo* toxicity is an open question. Our work contains a normal glial cell control, but addition of a normal mouse or human neural stem cell line as well as a neuronal line would serve as an important control. To a first approximation, we can perform an *in silico* counter-screen by comparing our data with the data of the Dirks laboratory at the University of Toronto [70]. While not comprehensive, this represents an important first step. Of note, zero compounds are in common, despite the libraries screened in both sets of experiments being quite

similar. Altogether, these data suggest that our candidate drug compounds identified by high-throughput screening are accurate, efficacious, and, at least to the level with which we can approximate *in vivo* cytotoxicity, safe for use in humans. Again, an important safety control is the fact that these compounds at one time or another were approved for use in humans. The critical test needed, which has is limited by time and money, is *in vivo* evaluation of each candidate compound in combination with the highly-penetrative polymeric nanocarrier. If we were to test each promising compound, the number of rats needed, including appropriate free drug controls, for an experiment with reasonable power, would stretch into the hundreds. The rigorously systematic approach utilized in discovering these compounds merits an equally systematic approach for *in vivo* testing. At present, we are unable to do this.

A critical question, which could be adequately addressed using clever RNAi-based methodologies but has not yet, is the ground state pathways needed for self-renewal and propagation of BCSCs. Pathway knowledge, in addition to being inherently interesting and possibly generalizable to cancer stem cells in other diseases, may also allow for rational design of drugs or improvement upon existing candidate compounds. To this end, a first approach might be to generate RNA expression array data from BCSC lines treated with various candidate compounds. In addition to providing knowledge about mechanism of action at the transcript or pathway level of a given individual compound, the set of data gleaned by comparing transcripts or pathways from different BCSC lines and multiple candidate drugs would allow for the definition of truly generalizable pathways. As the cost of collecting RNA

expression array data continues to decrease, this will one day be possible and standard practice for all candidate compounds.

Combined Role of Delivery System and Anti-BCSC Drugs in Treating GBM

After generating a BCSC-derived xenograft model of GBM in the rat that recapitulated the infiltrative nature of the native disease, we combined the results from our parallel drug delivery and drug discovery investigations to test whether CED of dithiazanine iodide-loaded highly-penetrative polymeric nanocarriers could inhibit tumor growth. We showed that the combination of a) a highly-penetrative polymeric nanocarrier-based controlled-release drug delivery system and b) a novel small molecule drug with *in vitro* efficacy against BCSCs resulted in a therapeutic that had an unprecedented ability to prolong survival of tumor-bearing rats. Altogether, this suggests that improved treatment of GBM might be achievable if obstacles pertaining to the infiltrative and chemoresistant properties of the disease can be sufficiently overcome.

Cancer Stem Cells

Based on the data presented in this thesis, we have argued convincingly for the combined roles of a BCSC-targeting drug and a highly-penetrative drug delivery vehicle. The latter of these is not particularly surprising: Of course more widespread controlled-release delivery of a drug should be beneficial. What was made clear in our experiments is that, at least in the context of a BCSC-derived xenograft rat model, the drug contained therein makes a huge difference. The previously

approved – and conventional chemotherapeutic – drug paclitaxel was used as a drug control in our early drug studies. We showed that widespread delivery of this compound was in no way sufficient to improve survival, while the addition of dithiazanine iodide to the highly-penetrative polymeric nanocarrier delivery vehicle was.

GBM represents a special case in oncology due to the unique delivery challenges associated with its location. It may not, however, be particularly unique in terms of its cellular hierarchy – this is the key lesson from our data, which provide more weight toward the cancer stem cell hypothesis (insofar as what we call "cancer stem cells" and what we isolate from GBM tumors using our state-of-the-art methods truly are the stem-like subpopulation of cells from a tumor responsible for the development of vasculature, proliferation of the tumor, and the significant invasion throughout the brain parenchyma.

While intertumoral genetic heterogeneity has become a very hot topic in the world of drug discover and drug development (as, essentially, the basis of personalized drug therapy), the extent to which intratumoral genetic heterogeneity must be addressed in drug discover and development remains to be seen. Fortunately, high-throughput small molecule screening has made possible the rapid evaluation of anti-proliferation effects of small molecule compounds. While not accounted for in this study, answering the question can be addressed simply with scaling.

An open question, of course, is the extent to which the BCSCs cultured

Recent mouse model evidence has added further force to the cancer stem cell hypothesis within GBM [86]. In studies of BCSCs, however, isolation of the cell lines

and subsequent *in vivo* modeling – and high-throughput small molecule screening – relies on culture of these cells in serum-free media. The effects culturing these cells have has not been quantified, but is likely to be significant. One possible future experiment to account for this effect is laser capture microdissection of the perivascular niche of these germ line-derived GBMs in mice. Genetic studies – from expression arrays, to sequencing, to methylation studies – and small molecule sensitivity studies would be possible, and neural stem cell controls in the contralateral subventricular zone provides for an excellent control.

Figures & Legends

Figure 1

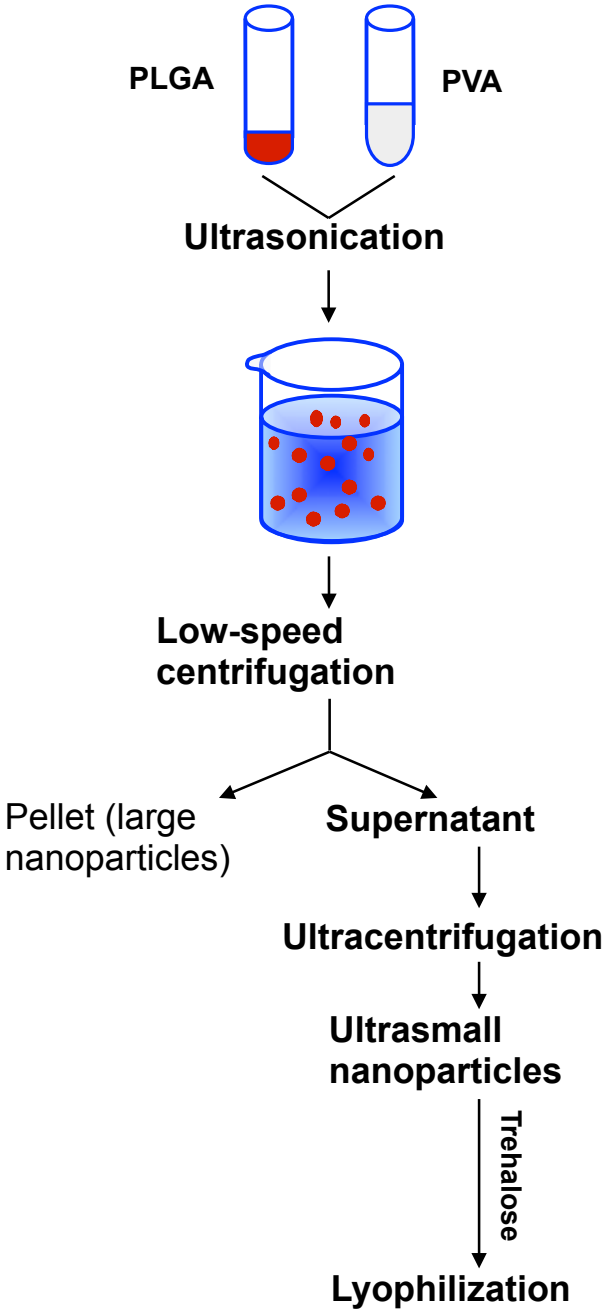

Figure 1. Method of fabrication of highly-penetrative polymeric nanocarriers. PLGA = poly(lactic-co-glycolic) acid; PVA = polyvinyl alcohol. Adapted from Zhou et al, 2013, *Proceedings of the National Academy of Sciences* [21].

Figure 2

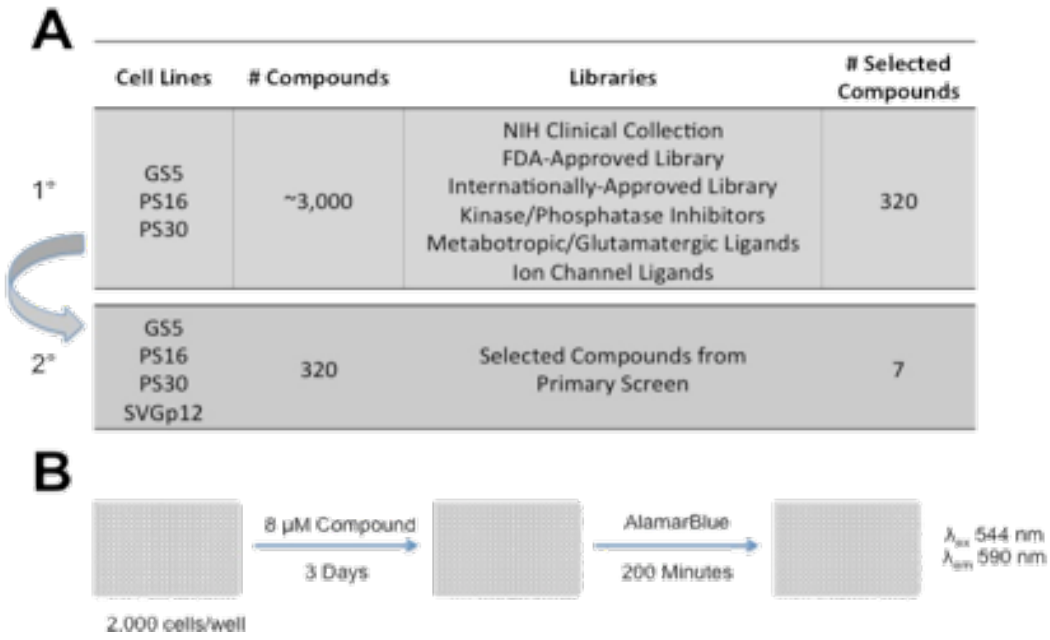

Figure 2. (A) Primary screening testing effects of ~3,000 compounds on three different BCSC lines. Top compounds were re-screened in BCSC lines and safety screened in normal glial cells SVGp12. (B) Basic schematic of screening protocol.

Figure 3

A

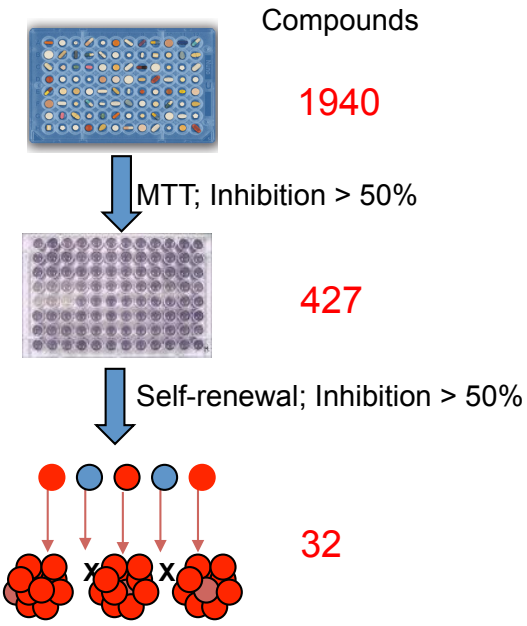

B

Test	GS5	PS11	PS16
IC50	79 nM	233 nM	62 nM
NS Inhibition (% Control)	93.6 ± 5.5%	91.2 ± 8.2%	99.7 ± 17.5%
CD133+ (% Control)**	56.6 ± 12.7%	58.7 ± 18.6%	18.2 ± 6.6%

Figure 3. Preliminary low-throughput in-house small molecule screen for anti-brain cancer stem cell compounds. Screening strategy with number of hits from each stage (A). Summary of cytotoxicity, self-renewal inhibition, and differentiation results of candidate compound dithiazanine iodide in three independently isolated brain cancer stem cell lines. Adapted from Zhou et al, 2013, *Proceedings of the National Academy of Sciences* [21].

Figure 4

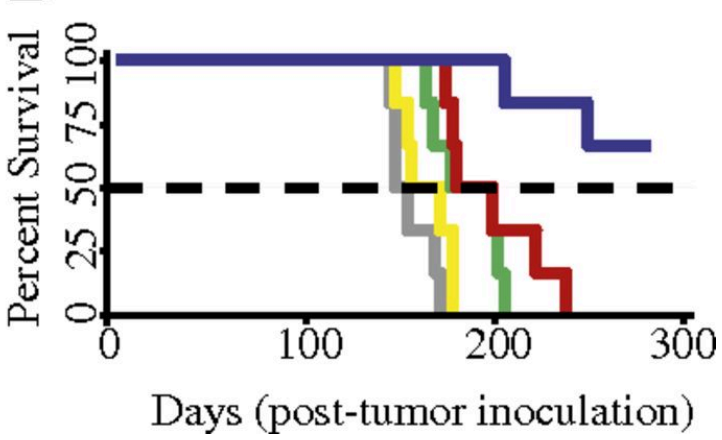

Figure 4. *In vivo* assessment of dithiazanine iodide-loaded ultrasmall nanoparticles in rats bearing brain cancer stem cell-derived xenograft tumors. Kaplan-Meier survival curve for dithiazanine iodide-loaded ultrasmall NPs (blue), dithiazanine iodide-loaded standard NPs (red), free dithiazanine iodide in solution (green), unloaded ultrasmall NPs (yellow), and no treatment (gray). Adapted from Zhou et al, 2013, *Proceedings of the National Academy of Sciences* [21].

Figure 5

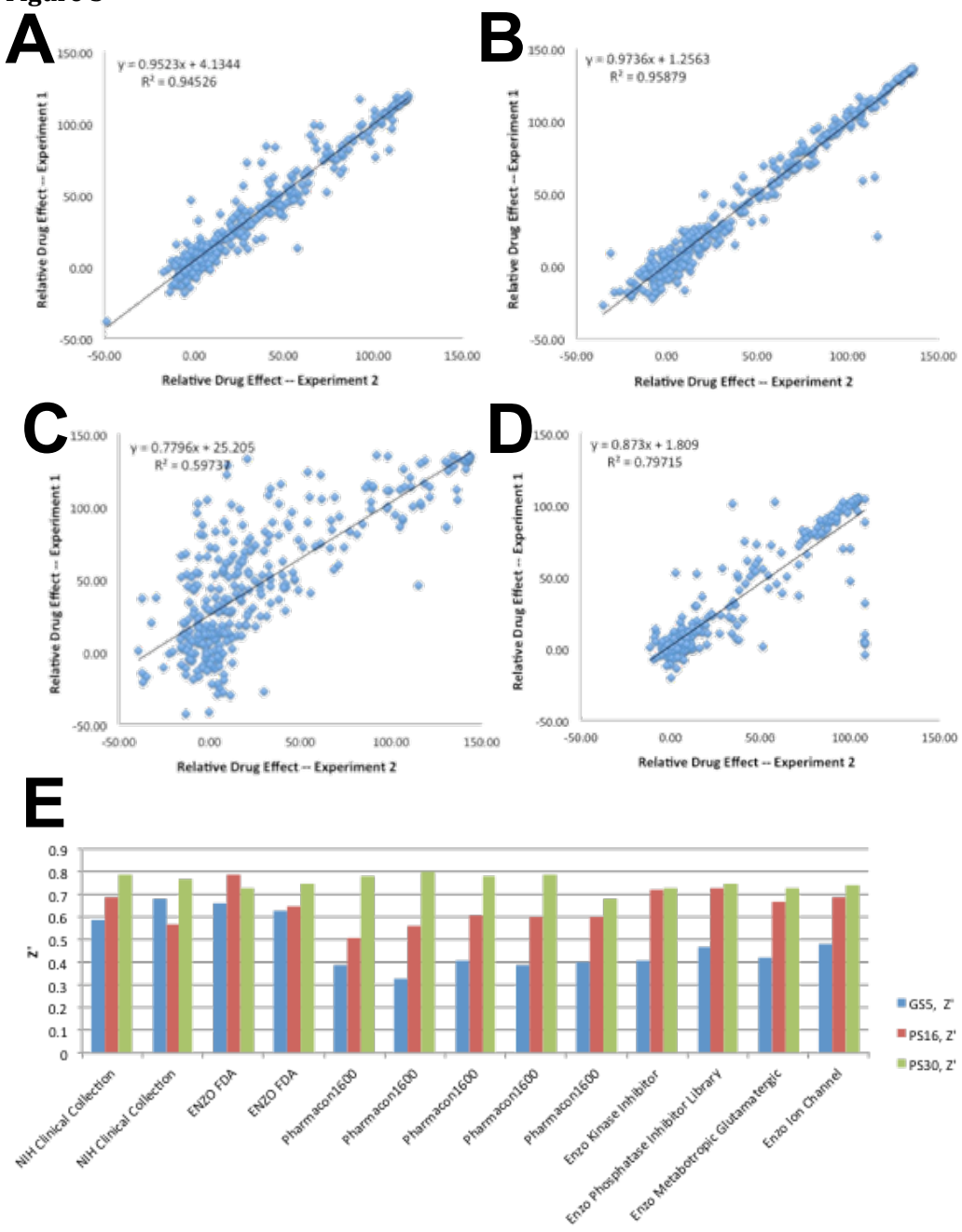

Figure 5. High-throughput small molecule screen quality control. 2D scatter plots of relative fluorescence intensity signals from two independent experiments in (A) GS5, (B) PS16, (C) PS30, and (D) SVGp12. (E) Plot of Z' values from primary screening in GS5 (blue), PS16 (red), and PS30 (green).

Figure 6

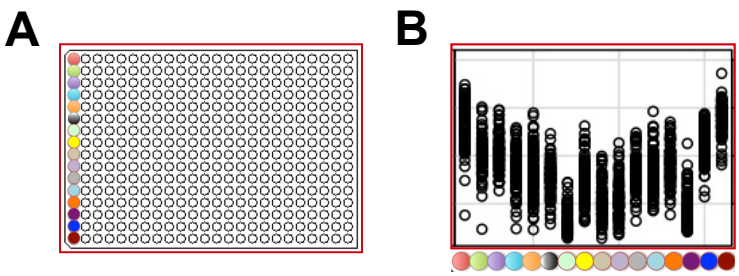

Figure 6. High-throughput small molecule screen quality control, summary of systematic plate effects. (A) Schematic of data, differentially colored wells refer to a given well. (B) Figure showing the luminosity of each row in a given column from a previous high-throughput screening project in BCSCs [71, 76].

Figure 7

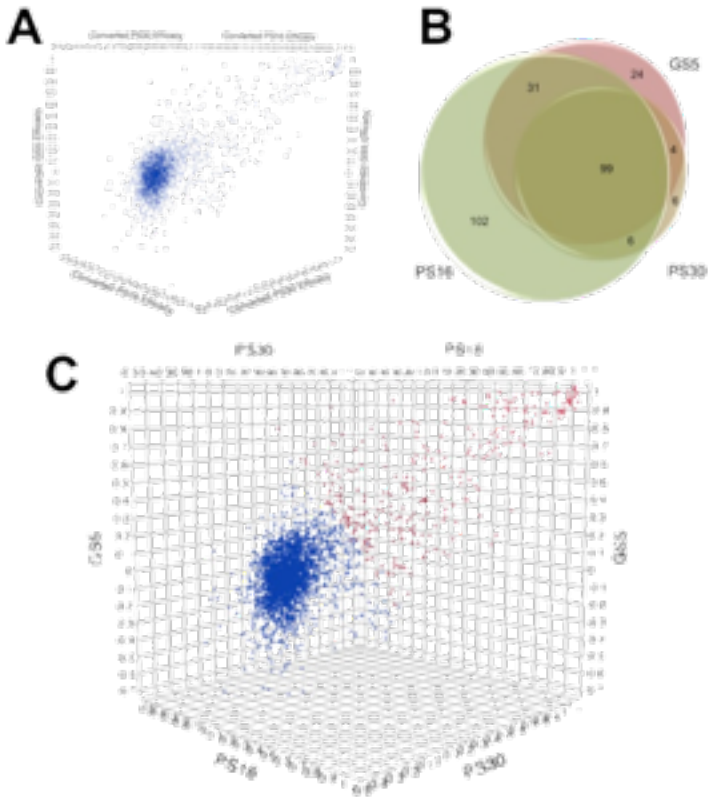

Figure 7. Primary high-throughput small molecule screening in brain cancer stem cell lines. (A) 3D scatter plot of relative efficacy results in GS5 (x), PS16 (y), and PS30 (z) cell lines. (B) Venn diagram showing overlap of cell line sensitivities to any drug with > 50% inhibition. (C) 3D scatter plot of relative efficacy results. Compounds chosen for secondary screening are in red.

Figure 8

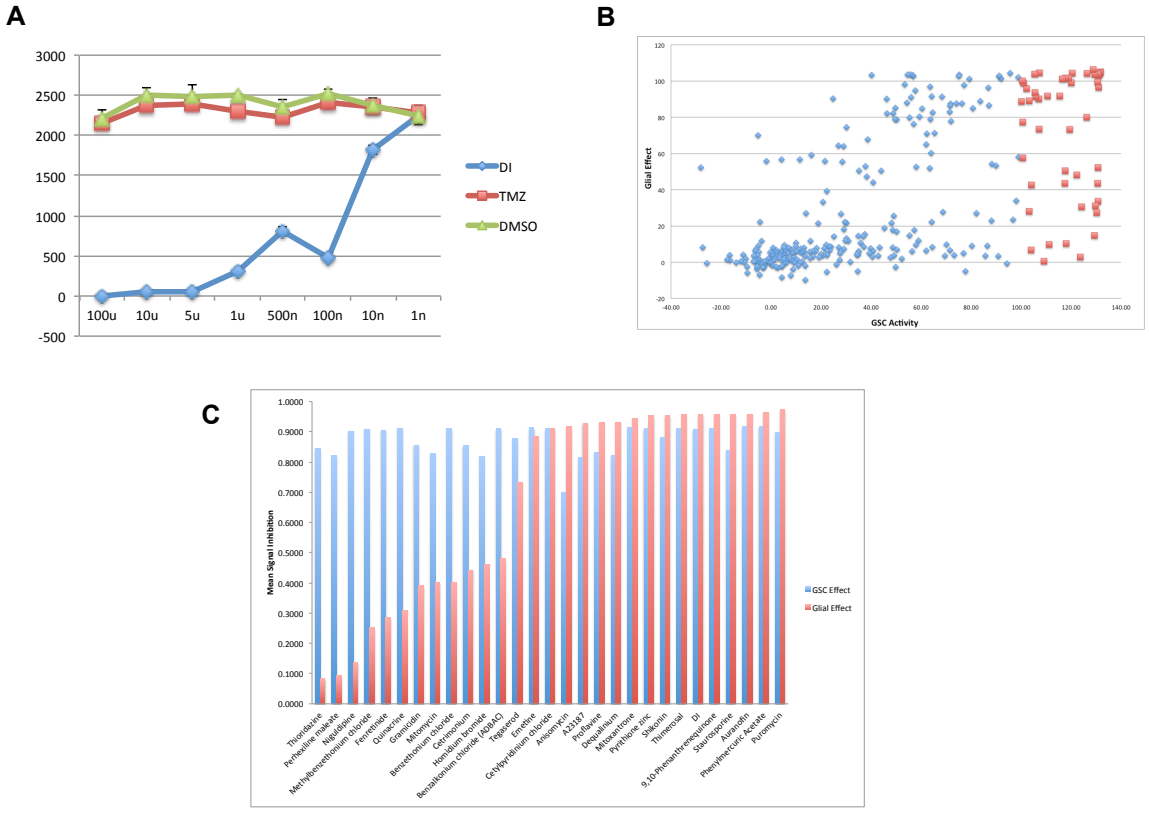

Figure 8. Counter-screening of candidate small molecule compounds against SVGp12 normal human glial cell line. (A) Percent of SVGp12 cells killed by candidate drug compound dithiazanine iodide at escalating doses, compared with temozolomide and DMSO vehicle controls. (B) Scatter plot of anti-glial cell toxicity versus mean anti-brain cancer stem cell anti-growth activity. Compounds in red, as most active against brain cancer stem cells, were highest-rated candidate compounds. (C) Compounds from (B) in red displayed as bar graph ordered by differential toxicity (anti-brain cancer stem cell activity – glial cell toxicity).

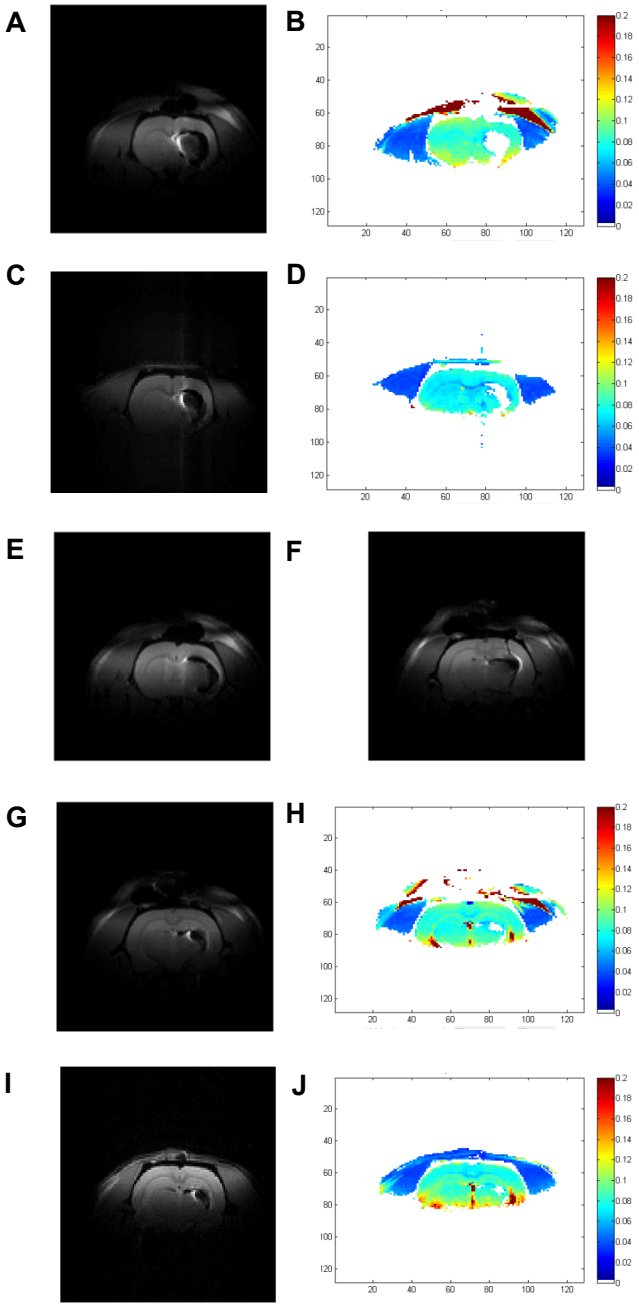

Figure 9. T1 MR imaging of superparamagnetic iron oxide-loaded highly-penetrative polymeric nanocarriers. High-volume infusate at time 0 (A-B) and time 28 days (C-D). Hyperdensities present in both A and C indicate position of nanoparticles. B and D are anatomically corresponding density maps of A and C. Though not present in this figure, saturation was present in the overall collection of

scans. “Bubbles” of volume associated with infusate and displaced brain tissue but not nanoparticles can be seen as black space (larger in E for high-volume and smaller in F for low-volume). T1 images for low-volume infusate at time of infusion (G) and one month (I), with hyperdensity again indicating nanoparticles. Anatomically corresponding density maps can be seen in H and J; owing to slight inter-procedural positional variation, saturation can be seen. Images between experiments (the sets A-D and G-J) are anatomically corresponding.

Tables & Legends

Histologic Grade	Name	Microscopy Findings
I	Pilocytic astrocytoma	Circumscribed, slow-growing tumor; eosinophilic granular inclusion bodies
II	Diffuse astrocytoma Oligodendroglioma Oligoastrocytoma	Infiltrative, slow-growing tumor; high cellularity but no mitoses Infiltrative tumor of "fried egg" cells; high cellularity but no mitoses Oligodendroglioma containing proliferative astrocytes
III	Anaplastic astrocytoma Anaplastic oligodenroglioma Anaplastic oligoastrocytoma	Diffuse astrocytoma with mitoses and hyperchromasia; no vascular proliferation or necrosis Oligodendroglioma with mitoses and vascular proliferation; no necrosis Oligoastrocytoma with mitoses and vascular proliferation; no necrosis
IV	Glioblastoma (GBM) Glioblastoma with oligodendroglial component (GBM-O)	Anaplastic astrocytoma with vascular proliferation and/or necrosis Anaplastic oligodendroglioma/ oligoastrocytoma with central necrosis

Table 1. World Health Organization Histologic Grading Criteria of Gliomas. Red text denotes gliomas of oligodendrocyte lineage while blue text denotes gliomas of astrocytic lineage. Microscopy findings typically noted on simple H&E staining. Ki67 index occasionally used for further information but is not an independent marker of grade.

Drug Name	Confirmed in UCLA Group Screen?
Quinacrine	N
Acriflavine	N
Cytarabine	N
8-Hydroxyquinidine	N
Digoxin	Y
Dithiazanine iodide	N
Neocuprine	N
Anisomycin	N
PAPP (4-Aminophenyl phosphate)	N
Betamethasone	Y
Chlorpheniramine	N
Proscillaridin A	N
BIBX 138	N
8Q1	N
PDTC (Ammonium pyrrolidinedithiocarbamate)	N
Iron (II) sulfate	N
Hydroxocobalamin	N
Glycocyamine	N
Calcium propionate	N
Miltefosine	N
Emetine	Y
Cladribine	N
Saponin	N
Parthenolide	N
Bromocriptine	N
Hycanthone	N
Prochlorperazine dimaleate	N
Astemizole	N
Harmine	N
Cephradine	N
Thioguanine	N
6-Mercaptopurine	N

Table 2. Compounds identified in in-house screening for anti-BCSC effects.

Small molecules with greater than 50% neurosphere inhibition and with greater than 50% proliferation inhibition. Identified compounds were compared to "finalist" compounds from Visnyei *et al,* Molecular Cancer Therapeutics, 2011. Only three compounds were also identified.

Drug	GS5	PS16	PS24	PS30	U87	GS5 (Hypoxia)
Digoxin	40.1 ± 13.9%	70.5 ± 2.7%	30.6 ± 5.6%	14.0 ± 5.4%	0 ± 0.9%	84.4 ± 2.3%
Acriflavine	92.9 ± 0.8%	85.3 ± 3.1%	94.5 ± 1.7%	83.1 ± 5.0%	95.5 ± 0.2%	82.8 ± 0.9%
Emetine	98.3 ± 0.3%	93.9 ± 4.8%	99.3 ± 1.4%	84.4 ± 1.7%	95.2 ± 0.3%	88.2 ± 0.7%

Table 3. *In vitro* efficacy characterization of candidate compounds identified in in-house screen. Percent inhibition values as calculated for digoxin, acriflavine, and emetine in five different cell lines under normoxic conditions and in the GS5 line under hypoxic conditions (90% O2, 5% CO2, and 5% N2). Notably, digoxin has only minimal anti-growth effects against bulk tumor cells, suggesting that if it is to be used as a therapeutic, it should be combined with a known inhibitor of bulk tumor cell growth such as BCNU, PCV, or temzolomide.

Drug	GS5	PS16	PS24	PS30	U87	GS5 (Hypoxia)
Digoxin	472 nM	38 nM	69 nM	82 nM	--	19 nM
Acriflavine	2.44 μM	1.29 μM	774 nM	1.50 μM	949 nM	502 nM
Emetine	134 nM	50 nM	51 nM	58 nM	14 nM	73 nM

Table 4. *In vitro* efficacy characterization of candidate compounds identified in in-house screen. Percent inhibition values as calculated for digoxin, acriflavine, and emetine in five different cell lines under normoxic conditions and in the GS5 line under hypoxic conditions (90% O2, 5% CO2, and 5% N2).

Compound ID	Mean BCSC Efficacy		SEM
YU034074	0.9176	±	0.0228
YU225107	0.9169	±	0.0236
YU226758	0.9136	±	0.0235
YU226560	0.9132	±	0.0241
YU227095	0.9126	±	0.0232
YU221339	0.9118	±	0.0224
YU033988	0.9114	±	0.0244
YU227090	0.9112	±	0.0235
YU226768	0.9109	±	0.0226
YU226510	0.9100	±	0.0234
YU226487	0.9099	±	0.0223
YU226751	0.9072	±	0.0219
YU224245	0.9041	±	0.0234
YU034420	0.9018	±	0.0237
YU224111	0.9003	±	0.0205
YU225125	0.8972	±	0.0209
YU221332	0.8821	±	0.0309
YU221036	0.8787	±	0.0232
YU226578	0.8694	±	0.0423
YU227152	0.8627	±	0.0692
YU226647	0.8619	±	0.0276
YU227021	0.8409	±	0.0406
YU154826	0.8385	±	0.0250
YU226471	0.8339	±	0.0314
YU227292	0.8328	±	0.0386
YU226739	0.8286	±	0.0568
YU225124	0.8253	±	0.0445
YU227165	0.8245	±	0.0362
YU221952	0.8232	±	0.0471
YU225073	0.8126	±	0.0583
YU224088	0.8113	±	0.0469
YU226361	0.7825	±	0.0556
YU040321	0.7786	±	0.0539
YU225086	0.7746	±	0.1440
YU226894	0.7631	±	0.0491
YU030802	0.7561	±	0.0560
YU225136	0.7553	±	0.0462
YU039604	0.7440	±	0.0453
YU039847	0.7437	±	0.1268
YU225128	0.7435	±	0.0538
YU221336	0.7415	±	0.0840
YU034048	0.7346	±	0.0783
YU226392	0.7345	±	0.0570
YU226869	0.7255	±	0.0529
YU039629	0.7213	±	0.0609
YU226852	0.7130	±	0.0666
YU039788	0.7127	±	0.0651
YU155446	0.7123	±	0.0582
YU154853	0.7044	±	0.0354

Table 5. Compounds with *in vitro* mean anti-BCSC efficacy greater than anisomycin. Compounds are ordered by mean efficacy, where efficacy is a number from 0 to 1, with 1 reflecting 100% killing of cells at 8uM dose and 0 reflection 0% killing of cells at the same dose. Notable is the number of compounds with efficacy reaching >90%, a number previously reached only by dithiazanine iodide, the only small molecule compound we have shown efficacious in an *in vivo* model of GBM.

References

1. Mrugala, M.M. and M.C. Chamberlain, *Mechanisms of disease: temozolomide and glioblastoma--look to the future.* Nat Clin Pract Oncol, 2008. **5**(8): p. 476-86.
2. Darefsky, A.S., J.T. King, Jr., and R. Dubrow, *Adult glioblastoma multiforme survival in the temozolomide era: a population-based analysis of Surveillance, Epidemiology, and End Results registries.* Cancer, 2012. **118**(8): p. 2163-72.
3. Frankel, S.A. and W.J. German, *Glioblastoma multiforme; review of 219 cases with regard to natural history, pathology, diagnostic methods, and treatment.* J Neurosurg, 1958. **15**(5): p. 489-503.
4. Larjavaara, S., R. Mantyla, T. Salminen, H. Haapasalo, et al., *Incidence of gliomas by anatomic location.* Neuro Oncol, 2007. **9**(3): p. 319-25.
5. Louis, D.N., H. Ohgaki, O.D. Wiestler, W.K. Cavenee, et al., *The 2007 WHO classification of tumours of the central nervous system.* Acta Neuropathol, 2007. **114**(2): p. 97-109.
6. Kleihues, P.a.O.H., *Primary and secondary glioblastomas- from concept to clinical diagnosis.* Neuro Oncol, 1999.
7. Parsons, D.W., S. Jones, X. Zhang, J.C. Lin, et al., *An integrated genomic analysis of human glioblastoma multiforme.* Science, 2008. **321**(5897): p. 1807-12.
8. Yan, H., D.W. Parsons, G. Jin, R. McLendon, et al., *IDH1 and IDH2 mutations in gliomas.* N Engl J Med, 2009. **360**(8): p. 765-73.
9. Hartmann, C., B. Hentschel, W. Wick, D. Capper, et al., *Patients with IDH1 wild type anaplastic astrocytomas exhibit worse prognosis than IDH1-mutated glioblastomas, and IDH1 mutation status accounts for the unfavorable prognostic effect of higher age: implications for classification of gliomas.* Acta Neuropathol, 2010. **120**(6): p. 707-18.
10. Balss, J., J. Meyer, W. Mueller, A. Korshunov, et al., *Analysis of the IDH1 codon 132 mutation in brain tumors.* Acta Neuropathol, 2008. **116**(6): p. 597-602.
11. Louis, D.N., *Molecular pathology of malignant gliomas.* Annu Rev Pathol, 2006. **1**: p. 97-117.
12. Hochberg, F.H. and A. Pruitt, *Assumptions in the radiotherapy of glioblastoma.* Neurology, 1980. **30**(9): p. 907-11.
13. Fan, X., L.G. Salford, and B. Widegren, *Glioma stem cells: evidence and limitation.* Semin Cancer Biol, 2007. **17**(3): p. 214-8.
14. Yu, S.C., Y.F. Ping, L. Yi, Z.H. Zhou, et al., *Isolation and characterization of cancer stem cells from a human glioblastoma cell line U87.* Cancer Lett, 2008. **265**(1): p. 124-34.
15. Li, Z., S. Bao, Q. Wu, H. Wang, et al., *Hypoxia-inducible factors regulate tumorigenic capacity of glioma stem cells.* Cancer Cell, 2009. **15**(6): p. 501-13.
16. Keith, B. and M.C. Simon, *Hypoxia-inducible factors, stem cells, and cancer.* Cell, 2007. **129**(3): p. 465-72.
17. Soeda, A., M. Park, D. Lee, A. Mintz, et al., *Hypoxia promotes expansion of the CD133-positive glioma stem cells through activation of HIF-1alpha.* Oncogene, 2009. **28**(45): p. 3949-59.

18. Liu, G., X. Yuan, Z. Zeng, P. Tunici, et al., *Analysis of gene expression and chemoresistance of CD133+ cancer stem cells in glioblastoma.* Mol Cancer, 2006. **5**: p. 67.
19. Kang, S.K., J.B. Park, and S.H. Cha, *Multipotent, dedifferentiated cancer stem-like cells from brain gliomas.* Stem Cells Dev, 2006. **15**(3): p. 423-35.
20. Jordan, C.T., M.L. Guzman, and M. Noble, *Cancer stem cells.* N Engl J Med, 2006. **355**(12): p. 1253-61.
21. Zhou, J., T.R. Patel, R.W. Sirianni, G. Strohbehn, et al., *Highly penetrative, drug-loaded nanocarriers improve treatment of glioblastoma.* Proc Natl Acad Sci U S A, 2013. **110**(29): p. 11751-6.
22. Chen, R., M.C. Nishimura, S.M. Bumbaca, S. Kharbanda, et al., *A hierarchy of self-renewing tumor-initiating cell types in glioblastoma.* Cancer Cell, 2010. **17**(4): p. 362-75.
23. Singh, S.K., I.D. Clarke, T. Hide, and P.B. Dirks, *Cancer stem cells in nervous system tumors.* Oncogene, 2004. **23**(43): p. 7267-73.
24. Bao, S., Q. Wu, R.E. McLendon, Y. Hao, et al., *Glioma stem cells promote radioresistance by preferential activation of the DNA damage response.* Nature, 2006. **444**(7120): p. 756-60.
25. Phillips, H.S., S. Kharbanda, R. Chen, W.F. Forrest, et al., *Molecular subclasses of high-grade glioma predict prognosis, delineate a pattern of disease progression, and resemble stages in neurogenesis.* Cancer Cell, 2006. **9**(3): p. 157-73.
26. Gerlinger, M., A.J. Rowan, S. Horswell, J. Larkin, et al., *Intratumor heterogeneity and branched evolution revealed by multiregion sequencing.* N Engl J Med, 2012. **366**(10): p. 883-92.
27. Sottoriva, A., I. Spiteri, S.G. Piccirillo, A. Touloumis, et al., *Intratumor heterogeneity in human glioblastoma reflects cancer evolutionary dynamics.* Proc Natl Acad Sci U S A, 2013. **110**(10): p. 4009-14.
28. Simpson, J.R., J. Horton, C. Scott, W.J. Curran, et al., *Influence of location and extent of surgical resection on survival of patients with glioblastoma multiforme: results of three consecutive Radiation Therapy Oncology Group (RTOG) clinical trials.* Int J Radiat Oncol Biol Phys, 1993. **26**(2): p. 239-44.
29. Reithmeier, T., E. Graf, T. Piroth, M. Trippel, et al., *BCNU for recurrent glioblastoma multiforme: efficacy, toxicity and prognostic factors.* BMC Cancer, 2010. **10**: p. 30.
30. Kappelle, A.C., T.J. Postma, M.J. Taphoorn, G.J. Groeneveld, et al., *PCV chemotherapy for recurrent glioblastoma multiforme.* Neurology, 2001. **56**(1): p. 118-20.
31. Buonerba, C., G. Di Lorenzo, A. Marinelli, P. Federico, et al., *A comprehensive outlook on intracerebral therapy of malignant gliomas.* Crit Rev Oncol Hematol, 2011. **80**(1): p. 54-68.
32. Brem, H., M.S. Mahaley, Jr., N.A. Vick, K.L. Black, et al., *Interstitial chemotherapy with drug polymer implants for the treatment of recurrent gliomas.* J Neurosurg, 1991. **74**(3): p. 441-6.
33. Brem, H., M.G. Ewend, S. Piantadosi, J. Greenhoot, et al., *The safety of interstitial chemotherapy with BCNU-loaded polymer followed by radiation*

therapy in the treatment of newly diagnosed malignant gliomas: phase I trial. J Neurooncol, 1995. **26**(2): p. 111-23.
34. Brem, H., S. Piantadosi, P.C. Burger, M. Walker, et al., *Placebo-controlled trial of safety and efficacy of intraoperative controlled delivery by biodegradable polymers of chemotherapy for recurrent gliomas. The Polymer-brain Tumor Treatment Group.* Lancet, 1995. **345**(8956): p. 1008-12.
35. Stupp, R., W.P. Mason, M.J. van den Bent, M. Weller, et al., *Radiotherapy plus concomitant and adjuvant temozolomide for glioblastoma.* N Engl J Med, 2005. **352**(10): p. 987-96.
36. Stupp, R., M.J. van den Bent, and M.E. Hegi, *Optimal role of temozolomide in the treatment of malignant gliomas.* Curr Neurol Neurosci Rep, 2005. **5**(3): p. 198-206.
37. Mellai, M., O. Monzeglio, A. Piazzi, V. Caldera, et al., *MGMT promoter hypermethylation and its associations with genetic alterations in a series of 350 brain tumors.* J Neurooncol, 2012. **107**(3): p. 617-31.
38. Hegi, M.E., A.C. Diserens, T. Gorlia, M.F. Hamou, et al., *MGMT gene silencing and benefit from temozolomide in glioblastoma.* N Engl J Med, 2005. **352**(10): p. 997-1003.
39. Wick, W., M. Weller, M. van den Bent, and R. Stupp, *Bevacizumab and recurrent malignant gliomas: a European perspective.* J Clin Oncol, 2010. **28**(12): p. e188-9; author reply e190-2.
40. Conley, S.J., E. Gheordunescu, P. Kakarala, B. Newman, et al., *Antiangiogenic agents increase breast cancer stem cells via the generation of tumor hypoxia.* Proc Natl Acad Sci U S A, 2012. **109**(8): p. 2784-9.
41. Stupp, R., M.E. Hegi, W.P. Mason, M.J. van den Bent, et al., *Effects of radiotherapy with concomitant and adjuvant temozolomide versus radiotherapy alone on survival in glioblastoma in a randomised phase III study: 5-year analysis of the EORTC-NCIC trial.* Lancet Oncol, 2009. **10**(5): p. 459-66.
42. Clarke, M.F., *Neurobiology: at the root of brain cancer.* Nature, 2004. **432**(7015): p. 281-2.
43. Kreuter, J., *Nanoparticulate systems for brain delivery of drugs.* Adv Drug Deliv Rev, 2001. **47**(1): p. 65-81.
44. Pardridge, W.M., *CNS drug design based on principles of blood-brain barrier transport.* J Neurochem, 1998. **70**(5): p. 1781-92.
45. Ostermann, S., C. Csajka, T. Buclin, S. Leyvraz, et al., *Plasma and cerebrospinal fluid population pharmacokinetics of temozolomide in malignant glioma patients.* Clin Cancer Res, 2004. **10**(11): p. 3728-36.
46. Smith, J.H. and J.A. Humphrey, *Interstitial transport and transvascular fluid exchange during infusion into brain and tumor tissue.* Microvasc Res, 2007. **73**(1): p. 58-73.
47. Baxter, L.T. and R.K. Jain, *Transport of fluid and macromolecules in tumors. I. Role of interstitial pressure and convection.* Microvasc Res, 1989. **37**(1): p. 77-104.
48. Baxter, L.T. and R.K. Jain, *Transport of fluid and macromolecules in tumors. II. Role of heterogeneous perfusion and lymphatics.* Microvasc Res, 1990. **40**(2): p. 246-63.

49. Baxter, L.T. and R.K. Jain, *Transport of fluid and macromolecules in tumors. IV. A microscopic model of the perivascular distribution.* Microvasc Res, 1991. **41**(2): p. 252-72.
50. Baxter, L.T. and R.K. Jain, *Transport of fluid and macromolecules in tumors. III. Role of binding and metabolism.* Microvasc Res, 1991. **41**(1): p. 5-23.
51. Bobo, R.H., D.W. Laske, A. Akbasak, P.F. Morrison, et al., *Convection-enhanced delivery of macromolecules in the brain.* Proc Natl Acad Sci U S A, 1994. **91**(6): p. 2076-80.
52. Allard, E., C. Passirani, and J.P. Benoit, *Convection-enhanced delivery of nanocarriers for the treatment of brain tumors.* Biomaterials, 2009. **30**(12): p. 2302-18.
53. Sampson, J.H., G. Akabani, G.E. Archer, M.S. Berger, et al., *Intracerebral infusion of an EGFR-targeted toxin in recurrent malignant brain tumors.* Neuro Oncol, 2008. **10**(3): p. 320-9.
54. Kunwar, S., S. Chang, M. Westphal, M. Vogelbaum, et al., *Phase III randomized trial of CED of IL13-PE38QQR vs Gliadel wafers for recurrent glioblastoma.* Neuro Oncol, 2010. **12**(8): p. 871-81.
55. Sampson, J.H., G. Archer, C. Pedain, E. Wembacher-Schroder, et al., *Poor drug distribution as a possible explanation for the results of the PRECISE trial.* J Neurosurg, 2010. **113**(2): p. 301-9.
56. Fahmy, T.M., P.M. Fong, A. Goyal, and W.M. Saltzman, *Targeted for drug delivery.* Materials Today, 2005. **8**(8): p. 18-26.
57. Muldoon, L.L., M. Sandor, K.E. Pinkston, and E.A. Neuwelt, *Imaging, distribution, and toxicity of superparamagnetic iron oxide magnetic resonance nanoparticles in the rat brain and intracerebral tumor.* Neurosurgery, 2005. **57**(4): p. 785-96; discussion 785-96.
58. Sawyer, A.J., J.K. Saucier-Sawyer, C.J. Booth, J. Liu, et al., *Convection-enhanced delivery of camptothecin-loaded polymer nanoparticles for treatment of intracranial tumors.* Drug Deliv Transl Res, 2011. **1**(1): p. 34-42.
59. Sawyer, A.J., J.M. Piepmeier, and W.M. Saltzman, *New methods for direct delivery of chemotherapy for treating brain tumors.* Yale J Biol Med, 2006. **79**(3-4): p. 141-52.
60. Neeves, K.B., A.J. Sawyer, C.P. Foley, W.M. Saltzman, et al., *Dilation and degradation of the brain extracellular matrix enhances penetration of infused polymer nanoparticles.* Brain Res, 2007. **1180**: p. 121-32.
61. Thorne, R.G., S. Hrabetova, and C. Nicholson, *Diffusion measurements for drug design.* Nat Mater, 2005. **4**(10): p. 713; author reply 714.
62. Hobbs, S.K., W.L. Monsky, F. Yuan, W.G. Roberts, et al., *Regulation of transport pathways in tumor vessels: role of tumor type and microenvironment.* Proc Natl Acad Sci U S A, 1998. **95**(8): p. 4607-12.
63. Zhou, J., T.R. Patel, M. Fu, J.P. Bertram, et al., *Octa-functional PLGA nanoparticles for targeted and efficient siRNA delivery to tumors.* Biomaterials, 2012. **33**(2): p. 583-91.
64. Sampson, J.H., M. Brady, R. Raghavan, A.I. Mehta, et al., *Colocalization of gadolinium-diethylene triamine pentaacetic acid with high-molecular-weight*

molecules after intracerebral convection-enhanced delivery in humans. Neurosurgery, 2011. **69**(3): p. 668-76.
65. Mardor, Y., O. Rahav, Y. Zauberman, Z. Lidar, et al., *Convection-enhanced drug delivery: increased efficacy and magnetic resonance image monitoring.* Cancer Res, 2005. **65**(15): p. 6858-63.
66. Bass, L.A., M. Wang, M.J. Welch, and C.J. Anderson, *In vivo transchelation of copper-64 from TETA-octreotide to superoxide dismutase in rat liver.* Bioconjug Chem, 2000. **11**(4): p. 527-32.
67. Plotkin, M., U. Gneveckow, K. Meier-Hauff, H. Amthauer, et al., *18F-FET PET for planning of thermotherapy using magnetic nanoparticles in recurrent glioblastoma.* Int J Hyperthermia, 2006. **22**(4): p. 319-25.
68. Pauleit, D., F. Floeth, K. Hamacher, M.J. Riemenschneider, et al., *O-(2-[18F]fluoroethyl)-L-tyrosine PET combined with MRI improves the diagnostic assessment of cerebral gliomas.* Brain, 2005. **128**(Pt 3): p. 678-87.
69. Rahmim, A. and H. Zaidi, *PET versus SPECT: strengths, limitations and challenges.* Nucl Med Commun, 2008. **29**(3): p. 193-207.
70. Diamandis, P., J. Wildenhain, I.D. Clarke, A.G. Sacher, et al., *Chemical genetics reveals a complex functional ground state of neural stem cells.* Nat Chem Biol, 2007. **3**(5): p. 268-73.
71. Visnyei, K., H. Onodera, R. Damoiseaux, K. Saigusa, et al., *A molecular screening approach to identify and characterize inhibitors of glioblastoma stem cells.* Mol Cancer Ther, 2011. **10**(10): p. 1818-28.
72. Himes, B.T., *Yale School of Medicine Thesis.* 2013.
73. Gunther, H.S., N.O. Schmidt, H.S. Phillips, D. Kemming, et al., *Glioblastoma-derived stem cell-enriched cultures form distinct subgroups according to molecular and phenotypic criteria.* Oncogene, 2008. **27**(20): p. 2897-909.
74. Ragheb, R.R., D. Kim, A. Bandyopadhyay, H. Chahboune, et al., *Induced clustered nanoconfinement of superparamagnetic iron oxide in biodegradable nanoparticles enhances transverse relaxivity for targeted theranostics.* Magn Reson Med, 2013. **70**(6): p. 1748-60.
75. Birmingham, A., L.M. Selfors, T. Forster, D. Wrobel, et al., *Statistical methods for analysis of high-throughput RNA interference screens.* Nat Methods, 2009. **6**(8): p. 569-75.
76. Sabatti, C.V., K.; Kornblum, H., *An introduction to statistical issues in high-throughput screens.* UCLA Statistics Department Preprint, 2008. **January**(#532).
77. Walters, J.H., *Infections of Immigrants.* Postgrad Med J, 1965. **41**(October).
78. Saleh, A., M. Schroeter, A. Ringelstein, H.P. Hartung, et al., *Iron Oxide Particle-Enhanced MRI Suggests Variability of Brain Inflammation at Early Stages After Ischemic Stroke.* Stroke, 2007. **38**(10): p. 2733-2737.
79. Saito, R., M.T. Krauze, C.O. Noble, M. Tamas, et al., *Tissue affinity of the infusate affects the distribution volume during convection-enhanced delivery into rodent brains: implications for local drug delivery.* J Neurosci Methods, 2006. **154**(1-2): p. 225-32.

80. Bar, E.E., A. Lin, V. Mahairaki, W. Matsui, et al., *Hypoxia increases the expression of stem-cell markers and promotes clonogenicity in glioblastoma neurospheres.* Am J Pathol, 2010. **177**(3): p. 1491-502.
81. Joshi, A.D., D.W. Parsons, V.E. Velculescu, and G.J. Riggins, *Sodium ion channel mutations in glioblastoma patients correlate with shorter survival.* Mol Cancer, 2011. **10**: p. 17.
82. Yip, K.W., X. Mao, P.Y. Au, D.W. Hedley, et al., *Benzethonium chloride: a novel anticancer agent identified by using a cell-based small-molecule screen.* Clin Cancer Res, 2006. **12**(18): p. 5557-69.
83. Gupta, P.B., T.T. Onder, G. Jiang, K. Tao, et al., *Identification of selective inhibitors of cancer stem cells by high-throughput screening.* Cell, 2009. **138**(4): p. 645-59.
84. Wurdak, H., S. Zhu, A. Romero, M. Lorger, et al., *An RNAi screen identifies TRRAP as a regulator of brain tumor-initiating cell differentiation.* Cell Stem Cell, 2010. **6**(1): p. 37-47.
85. Goidts, V., J. Bageritz, L. Puccio, S. Nakata, et al., *RNAi screening in glioma stem-like cells identifies PFKFB4 as a key molecule important for cancer cell survival.* Oncogene, 2012. **31**(27): p. 3235-43.
86. Chen, J., Y. Li, T.S. Yu, R.M. McKay, et al., *A restricted cell population propagates glioblastoma growth after chemotherapy.* Nature, 2012. **488**(7412): p. 522-6.